Journal of Agricultural Science; Vol. 16, No. 10; 2024
ISSN 1916-9752 E-ISSN 1916-9760
Published by Canadian Center of Science and Education

Assessing Remote Sensing-Based Maize Crop Biophysical Characteristics and Evapotranspiration Estimations

Zaid Al-Majali[1] & José Luis Chávez[1]

[1] Civil and Environmental Engineering Department, Colorado State University, Fort Collins, Colorado, USA

Correspondence: José Luis Chávez, Civil and Environmental Engineering Department, Colorado State University, Fort Collins, Colorado 80523-1372, USA. Tel: 1-970-491-6095. E-mail: jose.chavez@colostate.edu

Received: July 19, 2024 Accepted: August 20, 2024 Online Published: September 15, 2024

doi:10.5539/jas.v16n10p11 URL: https://doi.org/10.5539/jas.v16n10p11

Abstract

The rapid growth in population, climate variability, and decreasing water resources necessitate innovative agricultural practices to ensure food security and resource conservation. This study investigates the effectiveness of various multispectral imagery from remote sensing (RS) platforms, Unmanned Aerial Systems (UAS), PlanetDove microsatellites, Sentinel-2, Landsat 8/9, and proximal MSR-5 in assessing crop biophysical characteristics (CBPCs) and actual crop evapotranspiration (ETa) for maize fields in northeastern Colorado. The research aims to evaluate the accuracy of vegetation indices (VIs) derived from these platforms in estimating key CBPCs, including leaf area index (LAI), crop height (Hc), and fractional vegetation cover (Fc), as well as ETa. Field experiments were conducted during 2022 at the USDA-ARS Limited Irrigation Research Farm in Greeley, Colorado, U.S.A., using different irrigation strategies. Surface reflectance data collected using a handled sensor and observed LAI, Hc, and Fc values, served as ground truth for validating RS estimates. The study applied various statistical analyses to compare the performance of different RS platforms and models. Results indicate that higher-resolution platforms, particularly UAS, provided higher accuracy in estimating VIs and CBPCs than satellite platforms. The study also highlights the influence of environmental conditions on the accuracy of RS models, with locally calibrated models outperforming those developed in dissimilar conditions. The findings underscore the potential of advanced RS technologies in enhancing precision agriculture practices and optimizing water resource management.

Keywords: remote sensing, evapotranspiration, maize, irrigation water management

1. Introduction

The urgency of rapid population growth, climate variability, and dwindling water resources necessitates immediate and innovative approaches to enhance agricultural productivity while conserving natural resources. These pressing challenges underscore the critical need for sustainable farming practices that optimize resource use efficiency, mitigate environmental impact, and ensure food security for present and future generations (FAO, 2017). As the primary consumer of water among all water uses, irrigated agriculture, utilizing about 70% of the world's available water resources (Galán-Martín et al., 2017), is at the forefront of these challenges.

Improved irrigation water management is essential in ensuring water and irrigation sustainability (Sishodia et al., 2020; Ozdogan et al., 2010). Optimizing water use efficiency through drip irrigation or precision irrigation conserves water resources and minimizes water loss (Evans & Sadler, 2008). These techniques enhance crop productivity, support environmental conservation by reducing soil erosion and groundwater depletion, and help farmers adapt to changing climate conditions (Kumar et al., 2022; Atzberger, 2013). Additionally, efficient irrigation practices lead to economic savings and contribute to the long-term sustainability of agricultural systems, benefiting both present and future generations (Shanmugapriya et al., 2019).

Remote Sensing (RS) has emerged as a crucial tool in contemporary agricultural research, particularly in addressing water resource challenges (Karthikeyan et al., 2020). Its practical applications, such as facilitating the estimation of crop biophysical characteristics (CBPC) and actual crop evapotranspiration (ETa), enable more efficient irrigation water management and promise advancements in accuracy (Shanmugapriya et al., 2019; Moran et al., 1997). These advancements are critical to effectively addressing water resource challenges across diverse locations worldwide that vary in climate or topography. The accuracy of RS-based algorithms in estimating CBPCs is crucial, with key variables such as Leaf Area Index (LAI), Crop Height (Hc), and

Fractional Vegetation Cover (Fc) playing an important role in providing a quantitative measure of the vegetation health, structure, and distribution (Thenkabail et al., 2018; Wardlow & Egbert, 2008). These variables are fundamental in understanding the sophisticated dynamics of water use by crops, and their understanding enables informed decisions regarding water use applications by farmers, researchers, and policymakers (Sishodia et al., 2020).

In agricultural research, the study of CBPCs using RS has gained significance due to its implications for sustainable farming and natural resource management (Kingra et al., 2016). RS plays a pivotal role in estimating CBPCs and ETa, as it allows multispectral image data collection while providing frequent updates on changing crop conditions, offering high spatial and temporal resolutions for more detailed monitoring of these variables spatial variabilities (Bégué et al., 2018; Atzberger, 2013). Accurate estimation of ETa and CBPCs is crucial in appropriately estimating the water budget and provides a better understanding of water management in irrigated and rainfed crop fields (Olivera-Guerra et al., 2018; Facchi et al., 2013). RS-based products could indicate crop health, development, and growth, aiding in assessing crop development stages, predicting yields, and identifying stress factors (Karthikeyan et al., 2020). Proper spatially distributed ETa estimates can be used to better manage irrigation decisions, prevent water wastage, and sustainably use water resources, making the proper ET estimates a valuable tool in regions prone to drought or facing water scarcity challenges (Moran et al., 1997).

RS technologies offer numerous advantages when studying CBPCs and ETa (Calera et al., 2017). Firstly, they allow for large-scale and near real-time monitoring of agricultural areas, providing comprehensive spatial and temporal data, detecting changes over time, and assessing crop conditions in time and space. Secondly, RS techniques provide a non-invasive means of multispectral data collection, reducing the need for extensive fieldwork and physical measurements and resulting in a cost-effective tool (Kasampalis et al., 2018). The RS techniques save time and resources and enhance the accuracy and frequency of data collection, leading to more reliable insights and predictions (Wardlow et al., 2007). Moreover, RS facilitates the integration of multispectral and multitemporal images, enabling complex analyses and modeling of crop behavior and water dynamics, which enhances the understanding of ecosystem processes (Aeberli et al., 2021). RS data can also be used to assess the effectiveness of precision agriculture techniques and monitor changes in land cover, supporting informed strategies for sustainable farming and water resource management (Sishodia et al., 2020).

Many RS platforms are used to estimate CBPCs and ETa. The importance of choosing the proper platforms emerged dramatically to enhance the estimations of CBPCs, ETa, and other important factors related to crop growth and management (Jafarbiglu & Pourreza, 2022). Over the past two decades, there has been a substantial surge in the utilization of RS technologies, with a predominant focus on satellite platforms such as Landsat and Sentinel-2. Additionally, Unmanned Aerial System (UAS) technologies have significantly contributed to agricultural monitoring studies (Khanal et al., 2020), including ETa mapping (Chávez et al., 2020). In the context of irrigation water management (IWM), the utilization of RS, VIs, CBPCs, and ETa can substantially enhance operational efficiency and resource conservation. For instance, studies by Kamble et al. (2013) demonstrate the effectiveness of using satellite-based RS data to optimize irrigation scheduling. By integrating RS-derived VIs and surface temperature measurements, more accurate crop growth monitoring and water requirements lead to informed irrigation decisions (Chávez et al., 2024). In parallel, the analysis of ETa through RS-based methods offers real-time insights into crop water use dynamics (Saadi et al., 2018). Researchers can quantify ETa at field scales by analyzing RS multispectral image data, allowing for adaptive irrigation strategies that conserve water. Baret and Guyot (1991) emphasized that the accuracy of VIs is influenced by sensor calibration. They included the importance of accurate sensor calibration to ensure consistent and reliable VI values across RS platforms.

Many studies have developed VI-based models to estimate the CBPCs and ETa. Anderson et al. (2004) developed a VI-based model to estimate LAI and Hc, highlighting that the different RS platforms provide different VI values for the same observed crops and showing the importance of developing different calibration equations for estimating CBPCs. Also, Payero et al. (2004) compared eleven VIs for estimating the alfalfa and grass Hc, and the results showed the importance of selecting a suitable VI for a particular crop type and Hc.

Yang et al. (2015) used VI-based functions to estimate LAI, Hc, and Fc, Mourad et al. (2020) used various VIs to estimate LAI in semi-arid landscapes. Both studies highlighted the importance of different calibration equations for accurate CBPCs estimation, considering factors like sensor spatial resolution, spectral bands, and VI choices.

High accuracy for Hc estimation was achieved in a study by Costa-Filho et al. (2021) and Arslan et al. (2022), for instance. In those studies, the authors used empirical models based on LAI and the Normalized Difference Vegetation Index (NDVI) and found different calibrations for the Hc estimation. These results indicate how different site conditions and maize varieties can affect the Hc estimation results. Khaliq et al. (2018) and Jeong

and Park (2021) emphasized local-scale studies for accurate Hc estimation using VIs. Other studies, such as Bastiaanssen et al. (1998) and Vina et al. (2011), focused on LAI estimation incorporating multiple VIs to improve accuracy. Studies by Liu et al. (2011), Chávez et al. (2009), and Jayasree et al. (2013) demonstrated the advantages of higher-resolution multispectral data for more accurate LAI estimation. For Fc estimation, Johnson and Trout (2012) and Gitelson (2013) used NDVI-based models resulting with high coefficients of determination or R^2 values. Studies by Neale et al. (1989), Bausch (1993), and González-Piqueras et al. (2004) developed models for estimating the basal crop coefficient (Kcb) using various VIs. Singh and Irmak (2009) and Trout and DeJonge (2018) also focused on Kcb estimation, showing the importance of accurate VI-based models for crop water use estimation.

While numerous studies have developed and validated VI-based models for estimating CBPCs and ETa, there remains a need to evaluate the performance of these models across different RS platforms, especially with varying spatial and spectral resolutions. This research often focuses on specific environmental conditions, leaving a gap in understanding how these models perform in diverse settings, particularly semi-arid regions with different irrigation practices. Additionally, the impact of higher resolution on the accuracy of these estimates compared to lower satellite platforms has not been fully explored. This study aims to fill these gaps by evaluating the accuracy of VIs derived from various RS platforms in estimating CBPCs and ETa for maize in northeastern Colorado. By testing the hypotheses that higher-resolution RS multispectral data will yield more accurate estimates and that models developed under similar site conditions will perform better. Further, this research will contribute valuable insights into the optimal use of RS technologies for agricultural water management. The outcomes are expected to enhance precision agriculture practices and water resource management strategies, providing critical information for regions with similar environmental conditions.

2. Method

2.1 Site Description

The experiment was conducted in 2022 at the United States Department of Agriculture, Agricultural Research Service (USDA-ARS), Limited Irrigation Research Farm (LIRF) located in Greeley, Colorado, U.S.A. The study utilized two drip irrigated maize fields. In the eastern field, a deficit irrigation approach was implemented, subjecting the field to water stress conditions during the growth stages of the maize. Conversely, the western field was managed with a fully irrigated practice to maintain optimal soil water content levels throughout the growing season. This served as a comparative reference to evaluate the performance of maize under favorable irrigation conditions. The fields were situated at approximately Latitude 40.4470° N and Longitude -104.3696° W, with an elevation of around 1425 meters above mean sea level. Each of these fields has a rectangular shape of 190 × 110 m. Figure 1 below illustrates the precise location of the study area and provides a top view of the two studied fields.

2.2 Field Data Collection and Used Instruments

Proximal surface reflectance measurements were obtained using a portable multispectral radiometer (MSR5 CropScan, Inc., Rochester, MN, U.S.A.) at various stations throughout the maize growth season. The MSR5 radiometer is a compact handheld device that was mounted on a telescopic pole for nadir-looking measurements above the canopy. For each MSR5 radiometer measurement, the footprint was equivalent to a 1-meter-diameter circle over a ground sampling area. This passive sensor relies on natural sunlight and replicates Landsat-5 spectral bandwidths across the visible, near-infrared, and mid-infrared light spectrum. During this study, the MSR5 unit was used to take surface reflectance readings over 44 different stations within the study fields.

The LAI-2200C plant canopy analyzer, (Li-Cor, Inc., NE, U.S.A.) was used to measure maize LAI values. It accomplishes this by measuring radiation above and below the plant canopy and applying a theoretical relationship between leaf area and canopy transmittance. The optical sensor of this device consists of five detectors arranged in concentric rings, each detecting radiation below 490 nm from different portions of the sky. Canopy transmittance is calculated by comparing readings below the canopy to those above it for each detector ring. The leaf area estimate assumes that foliage elements are randomly distributed within the canopy.

The crop height was measured in situ, directly within the field where the crops were growing at the 44 sites. A tape measure was used to assess the height of the crops within their natural environment. These in-situ measurements ensured accurate and real-time data collection, reflecting the actual conditions of the crop at the time of measurement.

Weather conditions for the site area, as well as daily and hourly alfalfa reference evapotranspiration (ETr) data, were obtained from the COAGMET weather station Greeley 04 (GLY04), which was situated at the LIRF site

over well irrigated clipped grass. The station is positioned at a latitude of 40.449° N and longitude of -104.6380° W, northwest of the two study fields. Daily in-situ maize ETa data were obtained using an atmometer (Model E, ETgage, Loveland, Colorado, U.S.A.). The atmometer used in this study was composed of a Polyvinyl chloride (PVC) pipe placed around one meter above the ground. The PVC pipe is filled with distilled water, and information on the water used can be read by measuring the water drop daily. Atmometers consist of a porous, wet, ceramic cup placed on top of a cylindrical water reservoir. The ceramic cup is covered with a green canvas, simulating the canopy of maize (resistance). Distilled water is poured into the cylindrical reservoir, which evaporates from the ceramic cup and is pulled through a suction tube extending to the bottom of the reservoir. A special membrane underneath the fabric keeps rainwater from seeping into the cup. This atmometer (ETgage) was placed in the fully irrigated field only.

As for the Fc observations, the data were collected using the shadow sampling method, or as known, the meter-stick method. This method uses a meter stick that is placed on the land surface perpendicular to the crop rows. The length of the shadow on the stick is measured, and the ratio of the shadow length to the total length of the stick is the Fc, as indicated by (Adams & Arkin, 1997).

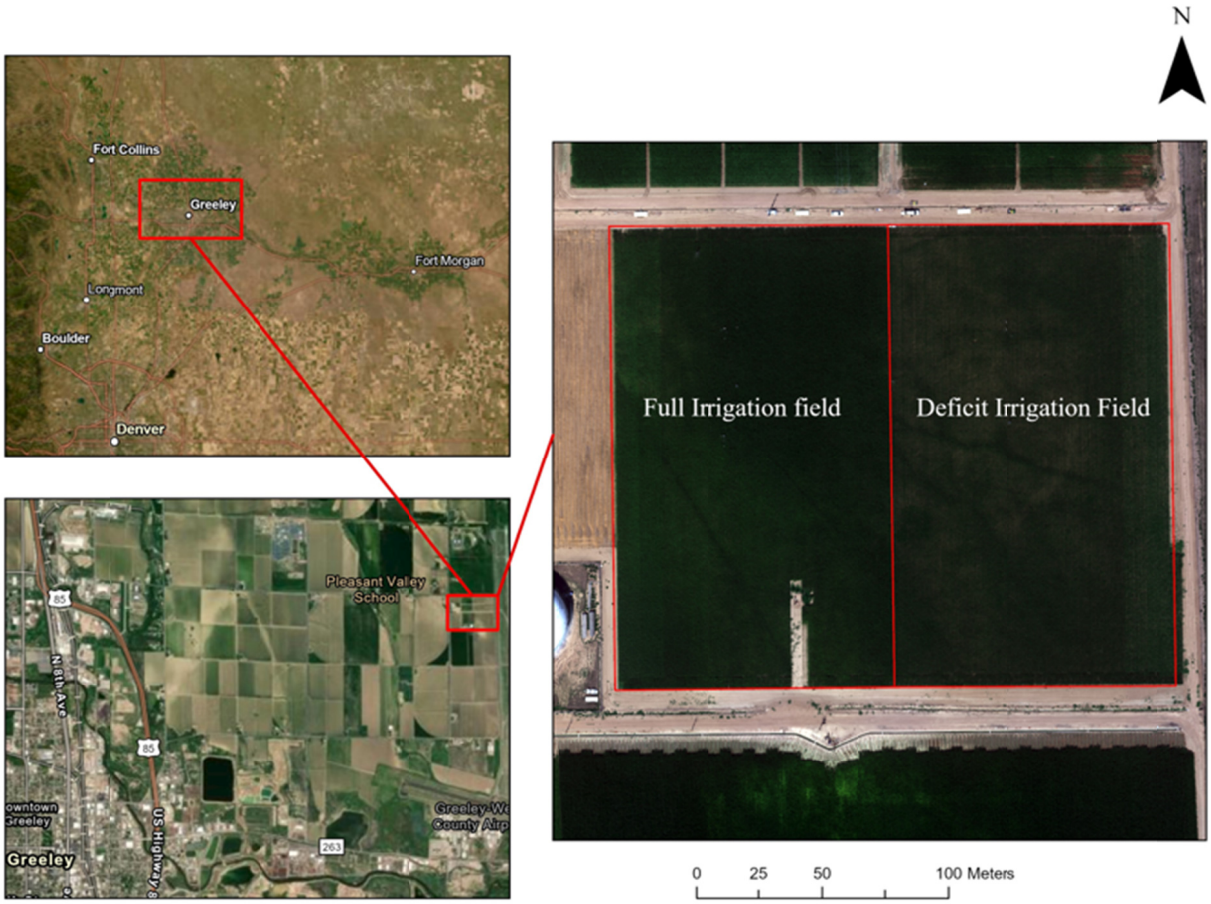

Figure 1. Location map of the study area near Greeley, Colorado, U.S.A.

2.3 Remote Sensing Data

As the main goal of this study was to compare and evaluate the performance of different RS platforms in estimating VIs, CBPCs, and ETa, this section introduces each of these platforms and provides some of their properties. Table 1. shows the general properties of each of these platforms.

2.3.1 The Unmanned Aerial System (UAS)

The UAS in this study was composed of a MicaSense RedEdge-MX multispectral camera (MicaSense Inc., Seattle, WA, U.S.A.), with five bands, including the visible and NIR bands. The UAS in this study acquired images over four separate flights at an elevation of 120 meters above field level.

2.3.2 PlanetDove Satellite

Planet Dove mini satellites are operated by Planet Labs (Planet Labs, Inc., San Fransisco, CA, U.S.A.). Planet is a low-cost commercial satellite constellation (150+) designed for frequent and global Earth imaging. The Dove satellites capture multispectral imagery at a resolution suitable for monitoring agricultural landscapes. The advantage of Planet Dove imagery lies in its high revisit rate and ability to provide consistent and up-to-date information on crop changes. The Planet surface reflectance images are pre-processed and calibrated with a factor of 10,000. Atmospheric corrections use MODIS data and the 6SV2.1 radiative transfer model (Planet team, 2017) to remove the effect of gases and aerosol concentrations and their changes in the altitude between the camera sensor in the space and the landscape. However, they exclude effects like stray light and haze from the correction process. Geometric corrections use sensor telemetry, ground control points, and digital elevation models to have a harmonized imagery version that meets the Sentinel-2 standards.

Table 1. Remote Sensing Platforms Characteristics

RS Platform	Spatial Resolution	Temporal Resolution	Used Bands	Central Wavelength (nm)	Band Width (nm)
UAS	0.03 meter	-	Red	668	14
			NIR	842	57
Planet	3 meters	1 day	Red	666	80
			NIR	867	80
Sentinel-2	10-60 meters	10 days	Red	665	31
			NIR	833	106
Landsat8/9	30-100 meters	16 days	Red	655	30
			NIR	870	30
			SWIR-2	2200	30
MSR-5	1 meter	-	Red	660	60
			NIR	830	140

2.3.3 Sentinel-2 Satellite

Sentinel satellites are part of the European Space Agency (ESA) Copernicus program, offering a series of Earth observation missions. Sentinel-2 has 2 satellites (Sentinel-2A and Sentnel-2B), and both provide multispectral images of the Earth's landscape. The radiometric resolution of the Sentinel-2 image is 16 bits after post-processing the images by the ESA from 12 bits. To provide surface reflectance images, the sentinel-2 images are pre-processed and calibrated through a calibration factor of 10,000; the ESA (Sen2Cor) developed an algorithm to process the atmospheric corrections.

2.3.4 Landsat 8/9 Satellite

It is a spaceborne RS platform operated by NASA and the USGS, providing the longest continuous global record of Earth's surface imagery. Landsat satellites take images of the land surface using the Operational Land Imager (OLI), which provides short-wave multispectral data, and the Thermal Infrared Sensors (TISS), which uses a camera to measure the long-wave infrared thermal radiation images. The radiometric resolution of Landsat imagery is 16 bits, converted from 12 bits after USGS/NASA post-process data. Linear calibration coefficients are used to convert the digital number (DN) to surface reflectance data.

2.4 Determination of Vegetation Indices

Four different RS-based VIs were calculated throughout the maize growth stages. These VIs include the NDVI, the Soil Adjusted Vegetation Index (SAVI), and the Optimized Soil Adjusted Vegetation Index (OSAVI), estimated based on surface Red and NIR reflectance data. The Normalized Difference Water Index (NDWI) was estimated but only for the MSR-5 and Landsat 8/9 platforms VIs. These VIs can be estimated using the following Equations 1 to 4:

$$NDVI = \frac{NIR - RED}{NIR + RED} \quad (1)$$

$$SAVI = (1 + L1)\frac{NIR - RED}{NIR + RED + L1} \quad (2)$$

$$OSAVI = (1 + L2)\frac{NIR - RED}{NIR + RED + L2} \quad (3)$$

$$NDWI = \frac{NIR - SWIR\_2}{NIR + SWIR\_2} \quad (4)$$

Where, NIR represents the target or surface reflectance in the near-infrared band, RED is the surface reflectance in the red band, and SWIR_2 is the Short-wave surface infrared reflectance. The L factor in Equation 2 and Equation 3 is the adjustment factor that has been used to minimize the interference caused by the soil background reflectance to the reflectance values from vegetated surfaces. The estimation of the L factor is based on crop densities. For SAVI, L1 was set to 0.5, and for OSAVI, L2 was set to 0.16.

The reflectance of the light for the maize surface was obtained using RED, NIR, and the Mid-Infrared (MIR) bands over 44 different stations, 22 stations in the fully irrigated field and 22 stations in the deficit irrigation field. Using ArcGIS Pro (ESRI, Redlands, CA, U.S.A.), circles or polygons representing Areas of Interest (AOI) were determined with a specific diameter of influence for each station. For the UAS and Planet images, an AOI diameter of 3 meters was used; for Sentinel-2, a 10-meter AOI diameter was used; and for Landsat images, a 30-meter AOI diameter was used. Each AOI was centered at the MSR-5 site coordinates. These different AOI diameters were set to capture the surface reflectance from the area of the pixel of interest. After a comprehensive collection of the reflectance data for each RS platform and each station throughout the dates mentioned, these reflectance data were used to estimate the VIs. These VIs were compared to the MSR-5 surface reflectance-based VIs data to evaluate the performance of each RS platform throughout the entire maize growth season.

2.4 Estimation of Crop Biophysical Characteristics

The LAI, Hc, and Fc were estimated using different functions based on different VIs. The CBPCs were estimated for each of the 44 stations. Several VI-based functions/models were tested for this study to estimate CBPCs. The selection criteria of CBPC calculation functions were based on using models that incorporated different site conditions, different RS platforms for measuring reflectance data, and various VI-based models. Firstly, site conditions variability may significantly impact the performance of VIs and RS platforms in estimating CBPCs. Secondly, different RS platforms (satellites, airborne, or proximal sensors) have varying spatial and spectral resolutions, which may influence the sensitivity and accuracy of VIs in estimating CBPCs. Additionally, different VIs respond differently to variations in CBPCs. Therefore, selecting different functions that align with the sensitivity and formulation of different VIs allows for a comprehensive evaluation of how these indices estimate CBPCs across diverse conditions and sensor types. Tables 2 to 4 show the selected models used to estimate the LAI, Fc, and Hc, respectively.

Table 2. Selected models for LAI estimation

Model-VI	Function	Reference
NDVI	$(VI + 1.1)(1 + 0.01 \cdot e^{5.72 \cdot VI})$	Mourad et al. (2020)
NDVI	$0.2092 \cdot e^{3.3554 * VI}$	Jayasree et al. (2013)
NDVI	$\log_{0.6}[(0.943 - VI)/0.731]$	Nguy-Robertson et al. (2012)
SAVI	$-[(1.49 \cdot \ln VI) + 2.71]/\ln VI$	
NDVI	$[\ln \frac{1}{1 - (\frac{VI - 0.2064}{0.7298})}]/0.6159$	Vina et al. (2011)
NDVI	$-\frac{[\ln 1.007 \cdot (1 - (1.036 \cdot VI))]}{0.719}$	Liu et al. (2012)
OSAVI	$-\frac{[\ln 1.123 * (1 - (1.155 \cdot VI))]}{0.562}$	
NDVI	$6.32 \cdot VI^{1.51}$	Yang et al. (2015)
SAVI	$-\frac{\ln \frac{0.69 - VI}{0.59}}{0.91}$	Bastiaanssen (1998)
OSAVI	$0.263 \cdot e^{3.813 \cdot VI}$	Chavez et al. (2009)
NDWI	$(2.88 \cdot VI + 1.14) \times (1 + 0.104 \cdot e^{4.1 \cdot VI})$	Anderson et al. (2004)
OSAVI	$(4 \cdot VI - 0.8) \times (1 + 0.00000473 \cdot e^{15.64 \cdot VI})$	

Table 3. Selected models for Fc estimation

VI-Based	Function	Reference
NDVI	$1.26 \cdot VI - 0.18$	Johnson and Trout (2012)
NDVI	$1 - (\frac{0.82 - VI}{0.74})^{0.696}$	Yang et al. (2015)
NDVI	$-[\ln (1 - \frac{VI}{0.93})]/3$	Gitelson (2013)

Table 4. Selected models for Hc estimation

Model-Based	Function	Reference
LAI	$\frac{LAI + 0.3919}{1.44}$	Arslan et al. (2022)
NDVI	$\frac{VI - 0.0285}{0.34}$	
NDVI	$0.283 \cdot VI - 0.0277$	Jeong and Park (2021)
NDVI	$3.4086 \cdot VI^{1.643}$	Yang et al. (2015)
LAI	$(0.697 \cdot e^{0.236 \cdot LAI}) - (3.42 \cdot e^{-3.177 \cdot LAI})$	Costa-Filho et al. (2021)
OSAVI	$(1.86 \cdot VI - 0.8) \times (1 + 0.000000482 \cdot e^{17.69 \cdot VI})$	Anderson et al. (2004)
NDWI	$(1.2 \cdot VI + 0.6) \times (1 + 0.04 \cdot e^{5.3 \cdot VI})$	
NDVI	$\frac{VI - 0.25}{0.21}$	Khaliq et al. (2018)

2.5 Estimation of Crop Coefficients and ETa

Multiple linear models based on Fc and VIs were used to estimate basal crop coefficients (Kcb). Table 5 shows the selected models used to estimate Kcb. The estimated coefficients were then used to estimate the daily maize actual evapotranspiration (ETa) using Equation 5.

$$ETa = Kcbx \cdot ETr \quad (5)$$

Where, *Kcbx* is the reflectance-based crop coefficient estimated by the *x* function shown in Table 5, and *ETr* is the daily alfalfa reference evapotranspiration calculated from observed COAGMET weather station data. The estimated daily ETa was compared to the daily ETgage estimated using in-situ measurements for the full irrigation field, shown in detail in section 2.2.

Table 5. Selected models for basal crop coefficient (Kcb) estimation

Model-Based	Function (Kcbx)	Reference
Fc	(1.1·Fc) + 0.17	Trout and DeJonge (2018)
NDVI	(1.181·NDVI) - 0.026	Neale et al. (1989)
SAVI	(1.416·SAVI) + 0.017	Bausch (1993)
NDVI	(1.2358·NDVI) + 0.0245	González-Piqueras et al. (2004)
NDVI	(1.308·NDVI) + 0.027	Singh and Irmak (2009)

2.6 Balanced Analysis

To ensure a balanced analysis, a new comparative study of the different RS platforms was carried out by selecting a subset of data acquired with the various platforms coinciding as closely as possible in overpass time. Given that there were only four UAS flights, the other platforms were matched with the dates of data acquisition of those of the UAS flights. The UAS-based data acquisition dates were July 21, July 25, August 18, and September 7. Table 6 presents the specific dates selected for each platform to ensure temporal alignment. The selected dates in Table 6 were used for the analysis to provide a clearer comparison of the results across different RS platforms. By focusing on these dates, we minimized the temporal discrepancies that could affect the accuracy of the comparative analysis.

Table 6. Dates of images chose for the balanced analysis

RS Platform	Dates
UAS	Jul/21, Jul/25, Aug/18, Sep/07
PlanetDove	Jul/17, Jul/27, Aug/18, Sep/07
Landsat	Jul/17, Jul/25, Aug/18, Sep/11
Sentinel-2	Jul/20, Jul/30, Aug/19, Sep/08
MSR-5	Jul/20, Jul27, Aug/18, Sep/07

To further balance the study and provide a comprehensive analysis, the data were separated into two distinct subsets representing early and late crop growth stages. This separation allows for the evaluation of the performance of the RS platforms and models across different developmental phases of the maize crop. The early growth stage was defined as the period from the beginning of the season until the end of July, while the late growth stage was defined as the period from the beginning of August until the end of the season. This approach ensures that the analysis covers different growth cycles of the maize crop and provides insights into how each RS platform performs at different stages.

2.6 Statistical Analysis, Models Performances, and Sensitivity Analysis

A One-way sensitivity analysis was done for all CBPCs and Kcb functions to assess the impacts of uncertainties of independent variables (VIs) on the output results of CBPCs and ETa estimates. The sensitivity analysis varied the value of the variable (*i.e.*, VIs, Fc, and LAI) in 2.5% (2.5% increase and 2.5 decrease) and 5% (5% increase and 5% decrease) increments. Any increase in VI values should yield a value less than or equal to one; since the values of the indices range between -1 and 1, any VI values larger than one were excluded. Also, an increase in Fc values should obtain an Fc value less than the expected maximum maize Fc of 85% (or 0.85), and any change in Fc values that results in an Fc value higher than 85% were excluded. As for the LAI changes, the values should not exceed 5.5 m^2/m^2, and any values exceeding 5.5 m^2/m^2 were excluded.

To evaluate the performance of the VIs and the selected CBPCs and ETa models, we utilized the Mean Bias Error (MBE), the Normalized MBE (MBE%), the Root Mean Square Error (RMSE), and the RMSE%. The MBE, MBE%, RMSE, and RMSE% are shown in Equations 6 to 9, respectively.

$$MBE = \frac{\sum Pi - Oi}{n} \tag{6}$$

$$MBE\% = \frac{MBE}{\bar{O}} \times 100\% \tag{7}$$

$$RMSE = \sqrt[2]{\frac{\sum (Pi - Oi)^2}{n}} \tag{8}$$

$$RMSE\% = \frac{MBE}{\bar{O}} \times 100\% \tag{9}$$

Where, Pi is the predicted value provided by the models, Oi is observed value, n is the number of observations (sample size), and $\bar{O}$ is the average value of the observed data.

The MBE helps assess prediction bias, where positive MBE values indicate overestimation and negative MBE values indicate an underestimation of the models compared to the observed data. The RMSE provides a measure of the overall prediction error. Lower values suggest better predictive accuracy relative to the scale of the actual values, while high RMSE values show that the model has high error. These metrics are commonly used in evaluating the performance of predictive models and are frequently employed to assess the effectiveness of predictive models. Jamieson et al. (1991) proposed the following categories based on RMSE% to evaluate the performance of the models (RMSE% ≤ 10%; Excellent performance, 10% < RMSE% ≤ 20%; Good performance, 20% < RMSE% ≤ 30%, Fair performance, RMSE% > 30%; Poor performance).

Before testing the function results, the data were subjected to a Median Absolute Deviation Analysis (MADA) to detect and remove outliers from the error analysis (Leys et al., 2013). The MADA was used in this study to replace the method used to remove the outliers based on using the mean and standard deviation. The MAD was calculated using the following equation:

$$MAD = b \times Mi(|xi - Mj(xj)|) \tag{10}$$

$$b = \begin{cases} 1.4826, & \text{normally distributed data} \\ 1/Q(0.75), & \text{non-normally distributed data} \end{cases} \tag{11}$$

Where, b is a constant linked to the normality of the data, Mi is the median of the new series that will be resulted by applying in between the brackets, xi is each individual value of the series, $Mj(xj)$ is the median of the original series. The process of this analysis is by subtracting each of the values of the original series with the median value of the original series, then find the median value of the new series, which resulted from the subtracting, and then multiplying the new median value with the constant b, finding the MAD value. After having the MAD value, the outliers can be detected by $M - 3 \cdot MAD < xi < M + 3 \cdot MAD$, All values greater than M + 3·MAD and smaller than M-3·MAD were excluded from the analysis. The use of (3·MAD) is suggested to be very conservative by Miller (1991) instead of using (2.5·MAD) or (2·MAD).

3. Results

3.1 Determination and Evaluation of Vegetation Indices

The VIs values from the satellite data were compared to the MSR-5 data-based VIs to evaluate the performance of each RS platform data quality. The performance of these indices was tested using Equation 6 to Equation 9. Table 7 shows the error analysis and performance of VI estimations.

As shown in the table below, the estimated VIs' performance using the UAS platform was excellent and higher than that of all other RS platforms. The better performance is likely due to the UAS's higher spatial resolution and the fact that the system acquired RS data closer to the land surface, thus minimizing atmospheric interference and capturing more detailed canopy information. The other RS platforms showed a relatively high performance in estimating VIs; they showed comparable trends in estimating VIs but with generally lower accuracies (higher MBE% and RMSE%) than the UAS, suggesting that they might be less sensitive to finer canopy details.

Table 7. Performance of VI estimations for each RS platform

RS platform	VI	MBE	MBE%	RMSE	RMSE%
UAS	NDVI	0.020	2.8	0.069	9.5
	OSAVI	-0.0002	-0.03	0.044	6.8
	SAVI	-0.026	-4.8	0.054	9.9
PlanetDove	NDVI	0.009	1.4	0.084	12.8
	OSAVI	0.034	6.0	0.078	13.5
	SAVI	0.004	0.8	0.067	13.7
Sentinel-2	NDVI	0.004	0.6	0.081	12.0
	OSAVI	-0.064	-11.0	0.102	17.3
	SAVI	-0.031	-6.3	0.081	16.4
Landsat	NDVI	0.021	3.1	0.081	11.5
	OSAVI	0.018	3.0	0.073	12.0
	SAVI	-0.007	-1.4	0.068	13.5
	NDWI	0.070	19.1	0.080	21.6

3.2 Estimation of CBPCs

3.2.1 Leaf Area Index Estimation Analysis

Based on Table 2, twelve models were selected to estimate the LAI; those models were based on different VIs. Table 8 shows the statistical analysis for each LAI function resulting from each RS platform studied.

The error analysis, conducted across a diverse range of functions and VIs for LAI estimation using different RS datasets, provides a comprehensive understanding of the performance and reliability of these models. The selected VIs, each with its unique characteristics, demonstrate varying degrees of performance across different studies and datasets. The NDVI was the most utilized index; however, SAVI and OSAVI demonstrated similar performance compared to NDVI. The performance of LAI estimation models was slightly influenced by the type of RS reflectance data used or the high spatial resolution; a slight better performance was noticed for the higher-resolution RS platforms. For instance, LAI results from models applied to PlanetDove, MSR-5, and UAS reflectance data showed relatively better performance compared to those applied to Landsat and Sentinel-2 data, which may provide evidence of how higher resolution RS platform can yield better estimations of LAI. The MBE values, which provide insights into the overall bias of the LAI estimation models, were predominantly negative, suggesting an underestimation of LAI and VIs estimations. The RMSE values reflect the accuracy of LAI estimation models throughout all the used models within all used RS platforms only. Mourad et al. (2022), Chavez et al. (2009), and Nguy-Robertson et al. (2012) models had a consistently high performance; these models were conducted in dry areas similar to weather conditions encountered in Greeley, CO, which shows the importance of selecting and applying LAI-functions developed for arid or semi-arid areas. On the other hand, LAI models by Liu et al. (2012), Bastiaanssen (1998), and Anderson et al. (2004) showed lower performance throughout all RS platforms. In Bastiaanssen's (1998) study, an overall function used to estimate the LAI for multiple crop types and in multiple countries was used, which resulted in poor performance across all RS platforms. This highlights the need for more specific and localized LAI estimation models. Also, Both Liu et al. (2012) study, conducted in Ottawa, Ontario, and Anderson et al. (2004), conducted in Walnut Creek Watershed, Iowa, had a humid site condition, significantly impacting the LAI results in this study. This emphasizes the importance of considering site conditions in future LAI estimation research.

Overall, higher-resolution RS platforms generally provide better performance, indicating that higher spatial resolution improves the accuracy of LAI estimation. Also, models developed in similar environmental conditions performed better, emphasizing the importance of site-specific calibration and the impact of differing site conditions on model accuracy. Moreover, the predominance of negative MBE values suggests a tendency for underestimation in LAI estimates across most models, which shows the need for further model calibration. In addition, model development localization is important, including the development of models with a specific crop type, crop variety, and sites. These key findings highlight the need for further research and development in the LAI estimation field, particularly in model calibration and site-specific considerations.

Table 8. Error analysis for LAI estimation models

Function	Landsat		Sentinel-2		Planet		UAS		MSR-5	
	MBE%	RMSE%	MBE%	RMSE%	MBE%	RMSE%	MBE%	RMSE%	MBE%	RMSE%
Mourad et al. (2022)	-2.9	20.8	3.5	18.6	0.2	19.3	8.5	19.6	7.2	22.8
Jayasree et al. (2013)	-20.5	28.5	-43.8	46.0	-17.7	25.1	-11.3	19.9	-15.4	24.8
Nguy-Robertson et al. (2012) (NDVI)	-17.0	26.9	-9.6	22.0	-14.1	24.0	-4.5	22.5	-9.6	26.2
Nguy-Robertson et al. (2012) (SAVI)	-7.6	20.0	-6.0	17.0	-1.5	19.7	10.6	27.1	-0.3	26.2
Vina et al. (2011)	-29.3	35.7	-22.4	29.7	-27.2	33.7	-15.4	26.1	-21.6	29.8
Liu et al. (2012) (NDVI)	-38.5	42.7	-34.7	38.3	-36.9	41.0	-30.2	33.7	-34.5	38.6
Liu et al. (2012) (OSAVI)	-34.0	38.2	-31.3	34.5	-29.4	34.6	-16.3	25.6	-25.8	33.3
Yang et al. (2015)	17.2	26.5	21.0	27.0	20.6	28.2	25.3	29.6	21.3	29.5
Bastiaanssen (1998)	-17.1	33.8	-20.8	32.3	-13.9	32.0	-18.5	31.8	-23.3	41.7
Chavez et al. (2009)	-8.2	21.5	-6.5	17.6	-3.5	19.5	5.9	20.7	-1.9	24.6
Anderson et al. (2004) (NDWI)	24.3	27.8	-	-	-	-	-	-	-3.6	19.2
Anderson et al. (2004) (OSAVI)	-36.0	42.0	-34.4	38.0	-33.5	38.9	-16.1	32.3	-27.7	37.0

A new analysis was done to estimate the LAI using each RS platform with closely coinciding overpass dates. This new study was done to balance the comparison between each RS platform by having similar/close dates, number of data points (days in time) compared. Table 9 shows the MBE% and RMSE% for the RS platforms used in this study.

The performance of different RS platforms in estimating the LAI varied considerably, as indicated by the MBE% and RMSE% metrics. The Landsat platform exhibited a wide range of performance across various models, suggesting that while Landsat can occasionally provide accurate LAI estimates, it has some limitations in accurately estimating the LAI for some models. Sentinel-2, on the other hand, demonstrated a slightly better overall performance than Landsat, indicating moderate reliability. Sentinel's ability to produce good performance metrics in certain models highlights its potential for more accurate LAI estimation under specific conditions. The Planet platform generally produced a fair performance, suggesting a slightly higher accuracy level. However, like Landsat and Sentinel, Planet's data showed variability, with many models exhibiting poor performance. UAS data consistently showed better performance across various models compared to other platforms. The best-performing models using UAS data achieved good performance levels with RMSE% values below 20%, and even the less accurate models generally fell within the fair range. This consistent performance underscores the higher accuracy and reliability of UAS for LAI estimation, likely due to its higher spatial resolution, flexibility in data acquisition, and proximity. The MSR-5 platform displayed mixed results, depending on the model used, suggesting that while MSR-5 can be useful, its performance is less consistent and generally lower than that of UAS for some models. Attention should be given to the type of RS data used in the development of given CBPC models. The UAS data provided the most reliable LAI estimates across different models, outperforming other RS platforms. Sentinel and Planet data showed moderate reliability, with potential for good performance in specific scenarios. Landsat generally exhibited higher variability and less reliability. MSR-5 demonstrated less consistent performance. These findings highlight the importance of choosing the appropriate RS platform based on the specific requirements and conditions of the study to ensure accurate LAI estimation.

The analysis of early and late crop growth stages reveals significant variations in the performance of the RS platforms in estimating LAI. By comparing the MBE% and RMSE% for each platform, this will allow showing the trends and identify which stages and platforms provide more accurate and stable results. During the early growth stages, the performance of RS platforms varied significantly. Generally, slightly higher RMSE% and MBE% values were observed, indicating less accuracy and greater bias in LAI estimates. For many RS platforms, the early-stage results exhibited considerable errors, reflecting the challenges associated with capturing accurate data during the initial phases of crop growth when the canopy is less developed and spectral signals are less accurate. Platforms like UAS, Planet, and MSR-5 demonstrated relatively better performance during the early stages compared to others. This suggests that in the early stages, with less dense canopies, the performance of higher spatial resolution RS platforms is higher since they capture the less dense vegetation more accurately without including the soil background, which will impact the results. In the late growth stages, the RS platforms generally exhibited improved performance compared to the early stages. This trend of improved performance in the late stages was consistent, especially for the lower spatial resolution RS platforms. The improved performance during the late stages can be attributed to the more stable and developed canopy structure, which

provides clearer spectral signals for the RS platforms to capture. The late growth stages generally provided better results across all RS platforms due to more stable canopy conditions. The UAS platform proved to be the most stable and dependable for LAI estimation, consistently showing moderate to good performance across both early and late stages. Sentinel also showed reasonable stability, particularly in the late stages, while platforms like Landsat and Planet exhibited higher variability and less consistent performance.

Table 9. Error analysis for LAI estimation models using balanced analysis

Function	Landsat		Sentinel-2		Planet		UAS		MSR-5	
	MBE%	RMSE%	MBE%	RMSE%	MBE%	RMSE%	MBE%	RMSE%	MBE%	RMSE%
Mourad et al. (2022)	-0.3	19.6	11.4	24.9	8.8	22.1	8.5	19.6	14.0	23.5
Jayasree et al. (2013)	-19.7	27.2	-39.1	41.9	-11.7	22.0	-11.3	19.9	-9.7	20.0
Nguy-Robertson et al. (2012)	-17.0	26.7	-3.7	26.7	-6.8	23.4	-4.5	22.5	-2.1	22.8
	-8.6	20.4	-6.6	17.5	6.7	20.6	10.6	27.1	9.6	26.2
Vina et al. (2011)	-28.7	34.4	-14.5	29.3	-19.5	28.6	-15.4	26.1	-15.6	24.6
Liu et al. (2012)	-37.3	41.1	-28.0	33.6	-30.9	36.1	-30.2	33.7	-29.7	33.5
	-34.1	38.0	-26.5	32.0	-22.4	28.2	-16.3	25.6	-19.0	27.4
Yang et al. (2015)	21.1	27.7	26.0	30.1	28.9	33.9	25.3	29.6	30.1	35.4
Bastiaanssen (1998)	-16.4	32.5	-20.2	34.7	4.7	33.1	-18.5	31.8	-15.2	40.7
Chavez et al. (2009)	-9.9	20.6	-2.4	22.5	4.8	19.3	5.9	20.7	8.5	24.6
Anderson et al. (2004)	26.8	29.5	-	-	-	-	-	-	1.5	16.7
	-39.5	42.7	-29.2	37.5	-26.0	32.8	-16.1	32.3	-20.2	31.8

3.2.2 Crop Height Estimation Analysis

Based on Table 3, eight models were selected to estimate Hc. Those models were based on different VIs and observed LAI values. Figure 2 shows the statistical analysis for each Hc function resulting from RS platforms used in this study. The findings of estimating Hc reveal that despite the variability of RS platform reflectance data, the relative performance of the used models to estimate Hc remained consistent. This consistency suggests that choosing a suitable function and VI- or LAI-based model is more critical than selecting a specific RS platform. As shown in the Figures below, better performance functions were based on OSAVI, NDWI, and observed LAI, which are crucial factors to consider. Furthermore, these high-performance LAI models have the same site conditions as LIRF, emphasizing the importance of choosing functions developed based on similar site conditions, including weather conditions, irrigation treatment, agricultural timing, and maize type. This understanding can significantly enhance the accuracy of canopy height estimations.

The highest performance of Hc estimation resulted from Costa-Filho et al. (2021) and Anderson et al. (2004) functions. Costa-Filho et al. (2021) model performed consistently well across all RS platforms with good performance and low RMSE%; this model appears to be the most reliable for estimating Hc in dry areas in Colorado or areas with similar weather conditions. The high performance in this study is interpreted by noting that the study was conducted at LIRF, showing the same weather conditions as this study. Anderson et al. (2004) functions that were based on using OSAVI- and NDWI to estimate the Hc showed higher performance across all RS platforms. On the other hand, the Hc estimation function by Khaliq et al. (2018), Arslan et al. (2022), and Yang et al. (2015) showed poor performance with an RMSE% exceeding 50%. The reason for the high error in these studies might be the type of RS sensor used and the maize genetic varieties that were different from the one used in this research. Different types of maize have different average canopy heights and structures. In the Arslan et al. (2022) study, silage maize was planted, and the function in this study was built on the Hc observed data, which exceeded 2.5 m height. As for Khaliq et al. (2018), the Hc function was based on ground observed data, which averaged 2.46 m.

Overall, estimating Hc using different RS platforms and models demonstrates the critical importance of model selection and calibration. The Costa-Filho et al. (2021) model provided reliable estimates, making it a preferred choice for Hc estimation in conditions similar to those encountered in Greeley. Conversely, models by Arslan et al. (2022) and Khaliq et al. (2018) showed poor performance, highlighting the need for site-specific models suitable to local conditions. This underscores the importance of considering environmental conditions and the specific characteristics of the RS platforms and models used in agricultural monitoring.

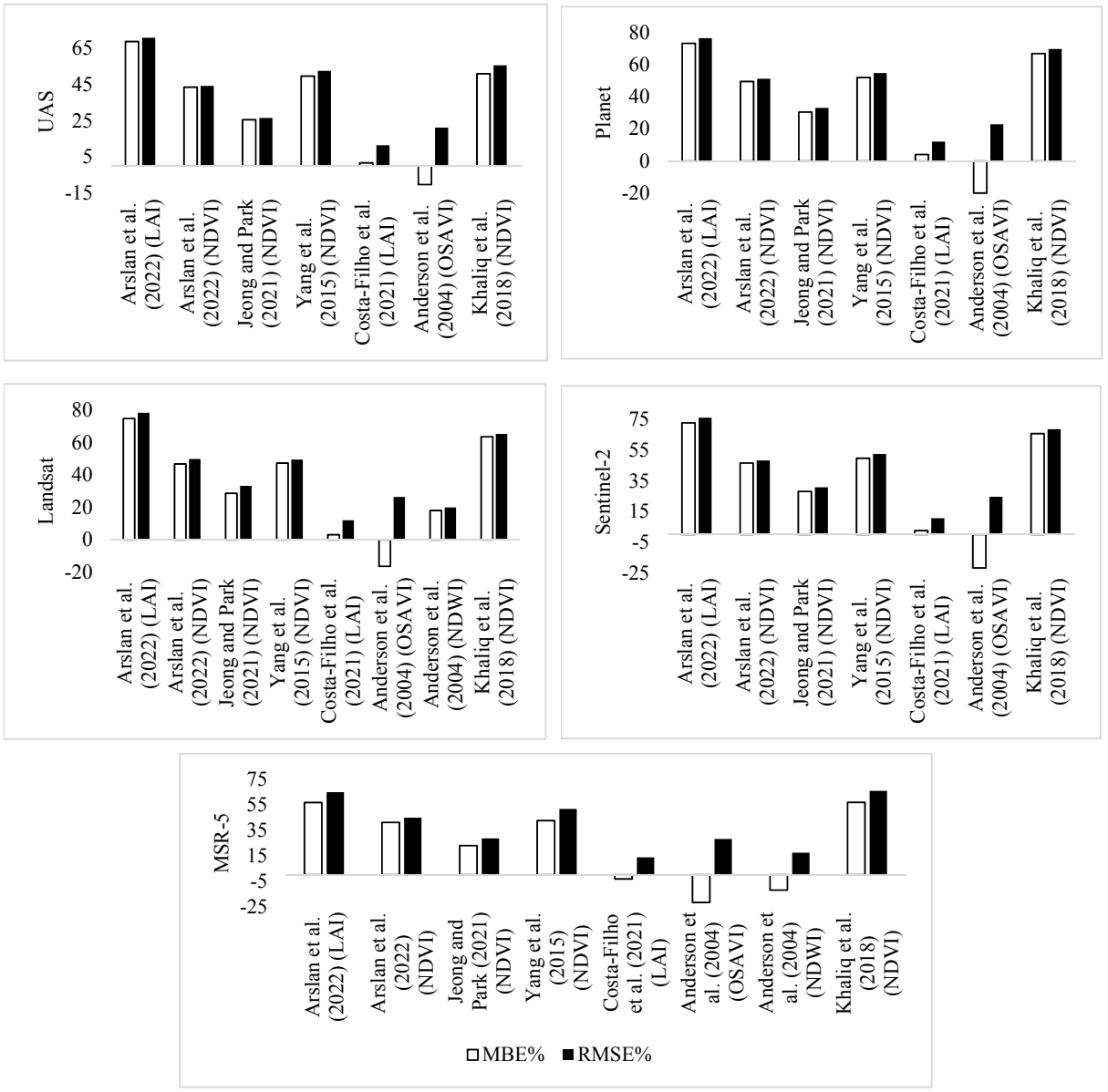

Figure 2. Error analysis for the Hc estimation

A new analysis was done to estimate the Hc using each RS platform with close dates. This was done to make the comparison between each RS platform more balanced by having similar/close dates and the same number of dates. Figure 3 shows the MBE% and RMSE% for the RS platforms used to estimate the Hc. The evaluation of various RS platforms for estimating Hc reveals distinct differences in performance and reliability. In this analysis, UAS showed a slightly better performance than the other platforms, with a generally lower RMSE%. However, the Landsat and Sentinel-2 platforms showed higher performances than the Planet and MSR-5 in estimating Hc. The evaluation of various RS platforms for estimating Hc reveals distinct differences in performance and reliability. The UAS showed a slightly better performance than the other platforms, with generally lower RMSE% values, indicating that UAS data is more accurate and reliable for Hc estimation. This higher performance can be attributed to the higher spatial resolution and its proximity, which allows for more detailed and precise measurements. On the other hand, and despite having a lower spatial resolution, Landsat and Sentinel-2 platforms showed higher performances than the Planet and MSR-5 in estimating Hc. The lower performance of the Planet and MSR-5 can be interpreted by noting that the tested models were developed using lower spatial resolution, such as ASTER images (15-meter spatial resolution) and Sentinel-2 (10-meter spatial resolution).

The analysis of early and late crop growth stages reveals significant variations in the performance of the RS platforms in estimating the Hc. During the early stages of crop growth, all the RS platforms had a similar trend, and their performance had a slight difference. In the late stages, the performance of the RS platforms did not significantly change except for the UAS, which demonstrated a significantly higher performance in estimating Hc during the late stages. Also, a slightly better performance for most utilized RS platforms was noticed.

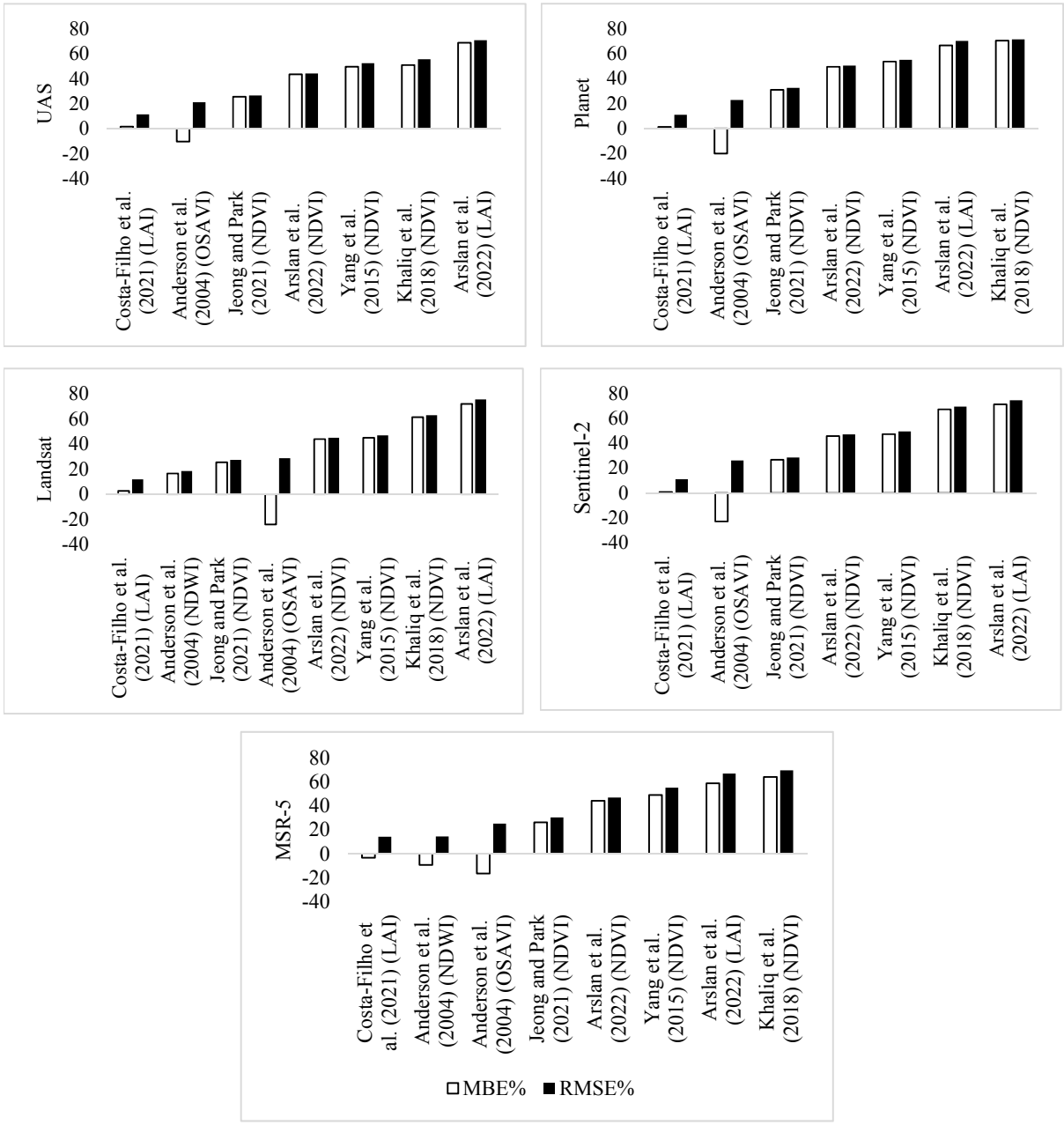

Figure 3. Error analysis for Hc estimation using balanced analysis

3.2.3 Fractional Vegetation Cover Estimation Analysis

Based on Table 4, three models were selected to estimate the Fc. Figure 4 shows the statistical analysis for each Fc function resulting from UAS, PlanetDove, Landsat, Sentinel-2, and MSR-5 RS platforms.

Consistent results and performance were noticed for all functions used to estimate Fc across all RS platforms. The UAS, which has the higher spatial resolution, showed a relatively higher performance in estimating Fc. However, Sentinel-2, which has a lower spatial resolution, did not show the lowest performance estimating Fc.

This suggests that factors other than spatial resolution, such as specific characteristics of the Fc models and their calibration, may play a significant role in the accuracy of Fc estimation. Across all platforms, the Gitelson (2013) model consistently demonstrated the lowest error values, indicating that it has more reliable results for estimating Fc. The model by Yang et al. (2015) showed relatively lower performance in estimating Fc than the other models, reflecting the importance of using models that developed in similar site areas, such as weather conditions, irrigation treatment, and maize type.

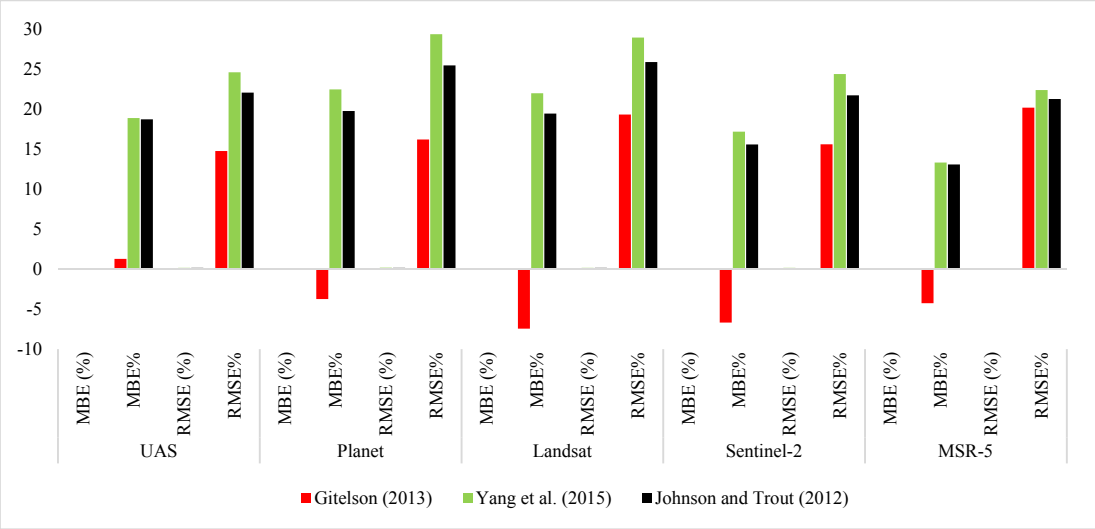

Figure 4. Error analysis for the Fc estimation

A new analysis was done to estimate Fc using each RS platform with acquisition dates close to each other. This was done to make the comparison between each RS platform more balanced by having similar/close data acquisition dates. Figure 5 shows the MBE% and RMSE% for the RS platforms used to estimate the Fc.

The UAS platform exhibited the highest performance in Fc estimation, characterized by consistently low MBE and RMSE values across different models, underscoring the reliability of UAS data, likely attributed to its high spatial resolution enabling detailed vegetation monitoring. Landsat data showed moderate to good performance in Fc estimation, suggesting that Landsat is a reliable option for Fc estimation for the crop growth stage covered. Sentinel-2 results also demonstrated strong performance, highlighting Sentinel-2's capability to provide consistent and accurate Fc estimates. In contrast, Planet and MSR-5 results showed more variability in Fc estimation. The higher RMSE values and greater variability in MBE% suggest that both Planet and MSR-5 results are less reliable for Fc estimation using the suggested models, potentially due to the models being developed using data from different RS platforms, leading to potential mismatches in sensor characteristics and data quality.

The analysis of early and late crop growth stages reveals significant variations in the performance of the RS platforms in estimating Fc. By comparing the MBE% and RMSE% for each platform, this will allow showing the trends and identify which stages and platforms provide more accurate and stable results. Table 27 shows the performance of UAS, Planet, Landsat, Sentinel-2, and MSR-5 platforms in estimating the Fc during the early and late stages of maize development. During the early growth stages, the higher spatial resolution platforms exhibited higher performance than the Landsat and Sentinel-2. However, all RS platforms showed higher error resulted during the early growth stages compared to the late stages. Platforms like UAS, Planet, and MSR-5 demonstrated relatively better performance during the early stages, suggesting that in early stages, the performance of higher spatial resolution RS platforms is better when the canopy cover is less dense, since they capture the less dense vegetation more accurately without including the soil background that will impact the results. In the late growth stages, all RS platforms exhibited better performance compared to the early stages. The improved performance during the late stages can be attributed to the more stable and developed canopy, which provides clearer spectral signals for the RS platforms to capture. The UAS platform proved to be the most stable and reliable for Fc estimation, which consistently showed higher performance across both stages. The Fc

models using Sentinel-2 and Landsat platforms showed a high improvement in the late stages, and slightly better performance using Planet and MSR-5 platforms.

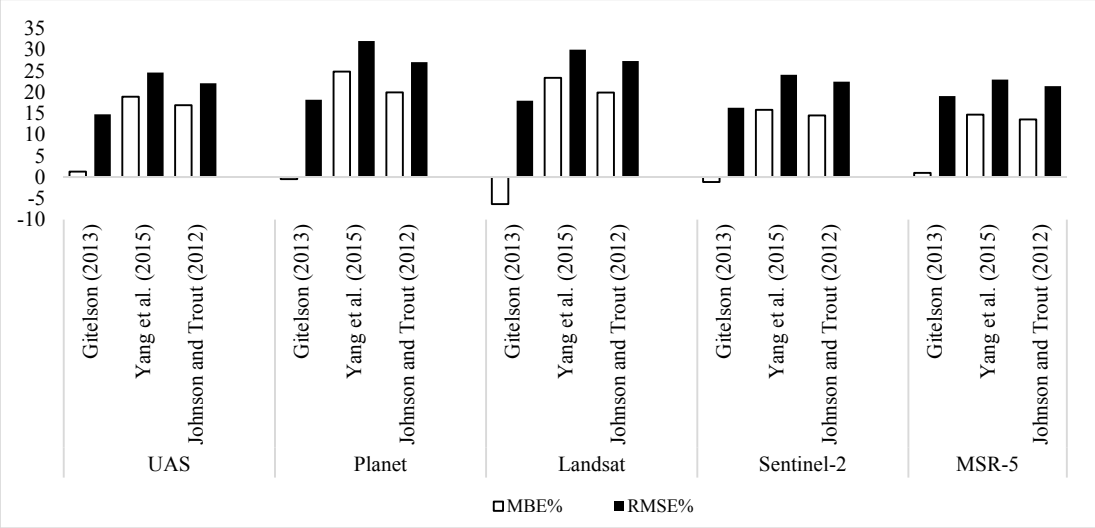

Figure 5. Error analysis for the Fc estimation using balanced analysis

3.3 Estimation of ETa

Based on Table 5, five RS-based ETa models were selected to estimate Kcb. Those models were based on different VIs or the fractional vegetation cover values estimated by Johnson and Trout (2012). After estimating the Kcb, the ETa was estimated using Equation 5. Figure 6 shows the statistical analysis (MBE and RMSE depicted by white and black bars respectively) for each ETa function resulting from each RS platform, compared to the ETgage 'measured' ETa values for the full irrigation field only. Just the fully irrigated field was instrumented with an ETgage atmometer.

All models performed well in estimating the ETa across all RS platforms. ETa estimations using the UAS and MSR-5 RS platforms showed the lowest RMSE%, showing that RS platforms with higher spatial resolution, and obtaining surface reflectance data closer to the ground, can perform better in estimating ETa. However, the results of PlanetDove functions failed to perform better than those of Landsat and Sentinel-2 platforms in estimating ETa despite its higher spatial resolution, which indicates that other factors, such as imagery atmospheric calibration and ET model calibration and site conditions, are also essential to be considered. The performance of models using inputs of VIs did not reveal a significant difference in estimating ETa. However, the model proposed by Trout and DeJonge, which utilized Fc as an input variable for ETa estimation, demonstrated a notably higher performance than other models, indicating a potential area for further research on the relationship between the Fc and ETa. The analysis also revealed that most models underestimated the ETa with negative MBE values. This shows the importance of continuous calibration of the models.

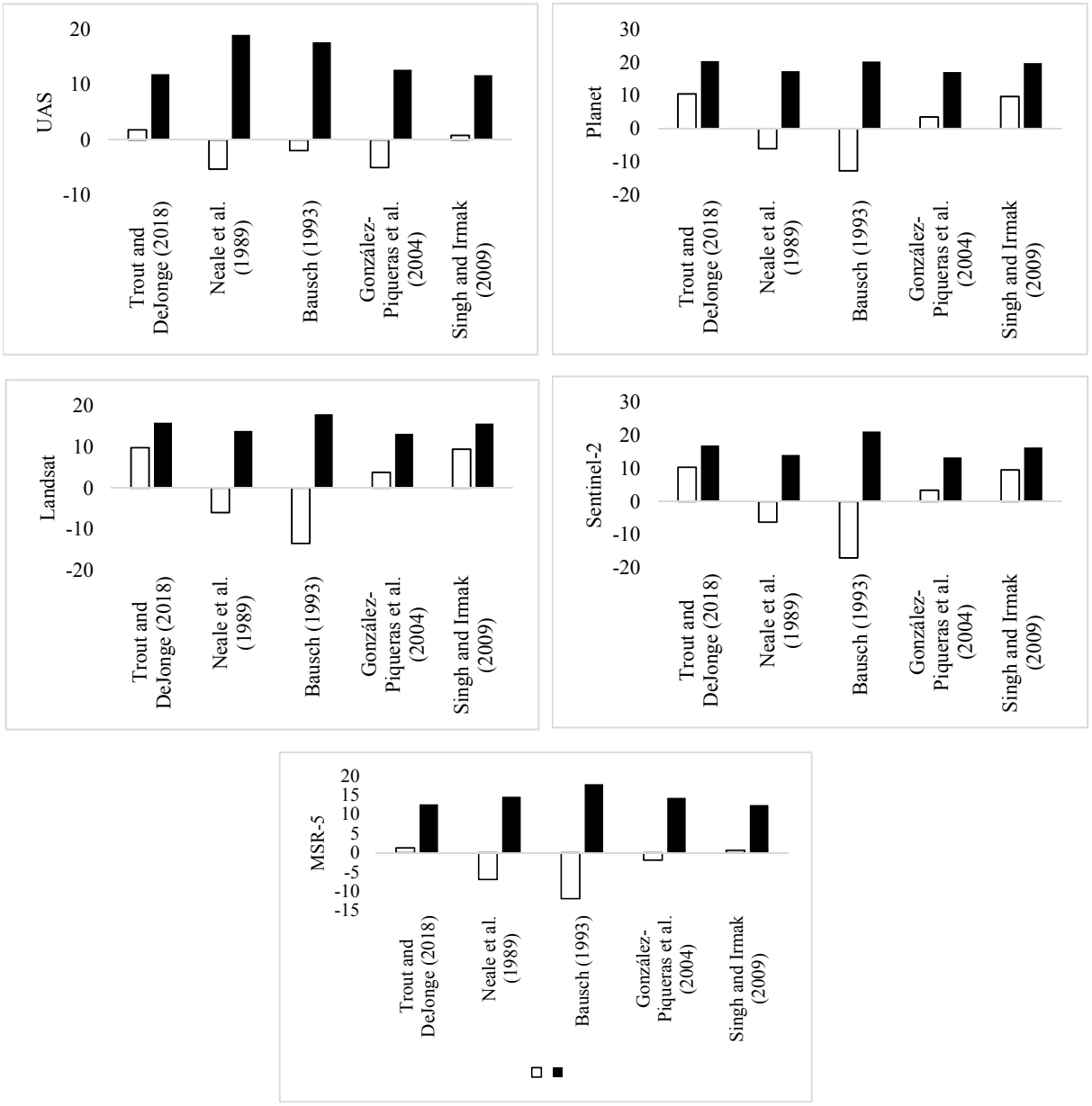

Figure 6. Error analysis for the ETa estimation

A new analysis was done to estimate the ETa using each RS platform with close dates. This was done to make the comparison between each RS platform more balanced by having similar/close dates. Figure 7 shows the MBE% and RMSE% for the RS platforms used to estimate the ETa.

Using the new balanced analysis, the UAS performance was slightly better than the other RS platforms in estimating ETa, highlighting the UAS's accuracy and higher spatial resolution. The Landsat and MSR-5 platforms also showed a high performance compared to the Sentinel-2 and Planet platforms, which showed lower performance in estimating ETa. The variations in performance among different RS platforms in estimating ETa can be attributed to differences in spatial resolution, sensor calibration, and the sensors used to develop the tested models. The UAS and MSR-5 were the most reliable platforms due to their high spatial resolution and proximity. Landsat showed higher performance due to the development of the models that were done using low spatial resolution sensors such as Landsat 5 and Landsat 7.

The analysis of early and late crop growth stages showed significant variations in the performance of the RS platforms in estimating ETa when comparing the MBE% and RMSE% for each platform in different stages. During the early growth stages, the performance of RS platforms varied significantly. Higher spatial resolution

platforms showed higher performance in the early stages, highlighting the importance of capturing accurate data during the initial phases of crop growth when the canopy is less developed and spectral signals are less accurate, with less dense canopies, the performance of higher spatial resolution RS platforms are higher, since they capture the less dense vegetation more accurately without including the soil background that will impact the results. In the late growth stages, the Landsat and Sentinel-2 RS platforms exhibited improved performance compared to the early stages, while other RS platforms did not show a significant change in performance. The higher performance during the late stages compared to the early stages can be attributed to the more stable and developed canopy, which provides clearer spectral signals for the RS platforms to capture. The UAS and Planet platforms had more stability in estimating ETa, showing moderate to good performance across both early and late stages. Sentinel-2 and Landsat showed lower stability.

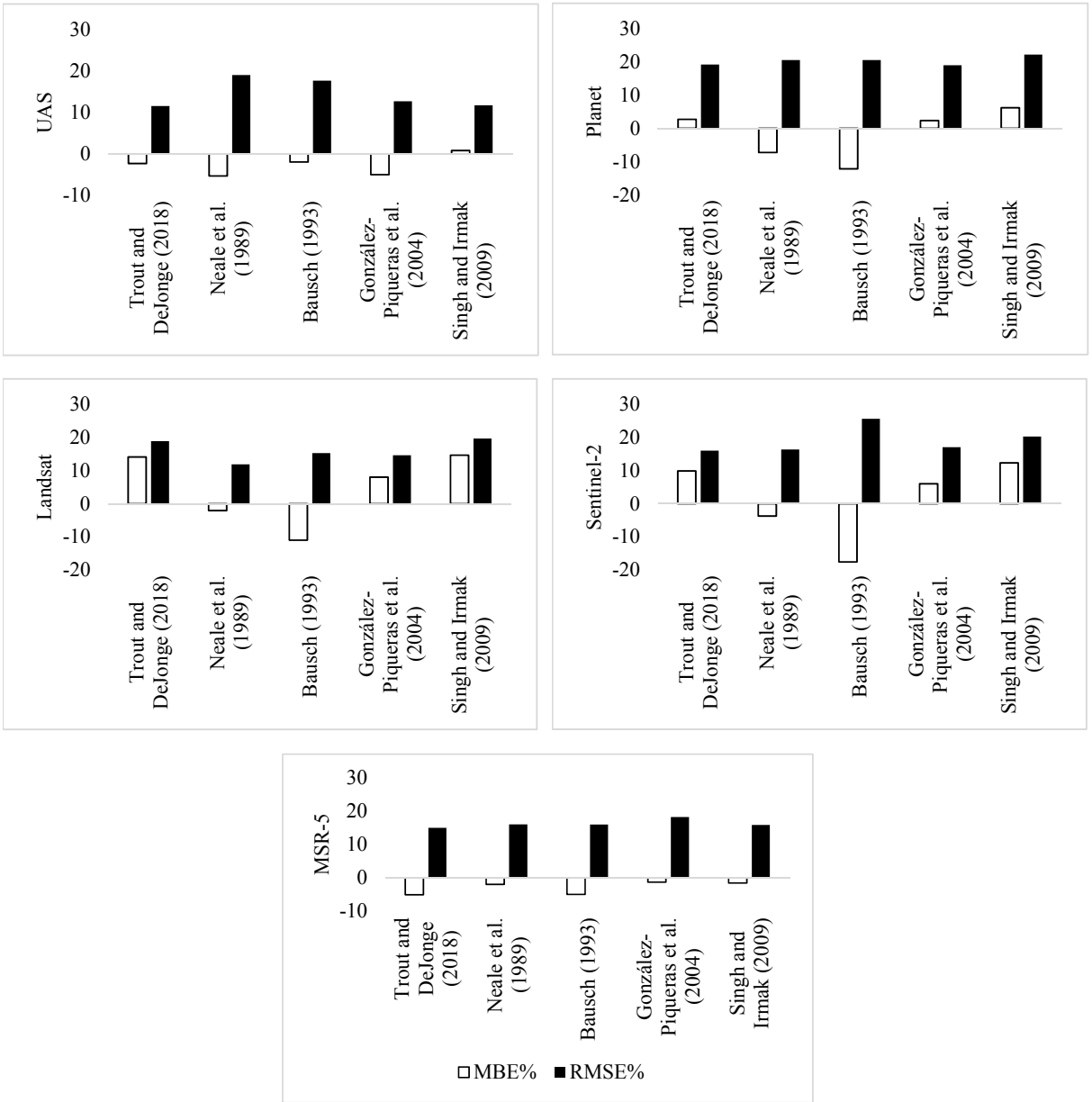

Figure 7. Error analysis for the ETa estimation using balanced analysis

3.4 Sensitivity Analysis

3.4.1 Leaf Area Index Estimation Analysis

A sensitivity analysis for the estimation of LAI, Hc, Fc, and ETa was done using four different scenarios, including +2.5%, +5%, -2.5%, -5% variation of the values of the independent variables. The analysis was done for all RS platforms to indicate how different VI values will impact the dependent LAI value. Figure 8 and Figures A1 to A4 in Appendix A show the RMSE% for the base models and how changes in VI values impact the RMSE% of the models for the UAS, PlanetDove, Landsat, Sentinel-2, and MSR-5 platforms, respectively.

The sensitivity analysis for the UAS platform in estimating LAI shows that the models are relatively stable, with RMSE% ranging from 15.95% to 39.62%. The slight increase in RMSE% under positive scenarios indicates that the model tends to overestimate LAI slightly when VIs increase. Conversely, the models show less deviation in RMSE% under negative scenarios, suggesting better performance in estimating lower LAI values. The PlanetDove platform, however, exhibits a broader range of RMSE%, indicating a higher sensitivity to changes in VI values, particularly under negative scenarios, where the RMSE% increases significantly. The results suggest that while PlanetDove can effectively estimate LAI, it is more susceptible to inaccuracies when there is a decrease in VI values. The sensitivity analysis for Landsat shows RMSE% variations similar to those of the UAS platform, exhibiting moderate sensitivity to VI changes, with slightly higher RMSE% under positive scenarios. Sentinel-2, on the other hand, demonstrates a more comprehensive RMSE% range, indicating higher sensitivity than the UAS and the Landsat platforms. The analysis shows significant variations under both positive and negative scenarios, suggesting that Sentinel-2 is sensitive to both increases and decreases in VI values, impacting the accuracy of LAI estimates. The MSR-5 platform shows the highest sensitivity; the significant variation in RMSE% indicates that MSR-5 is highly sensitive to changes in VI values, particularly under negative scenarios, where the RMSE% increases drastically.

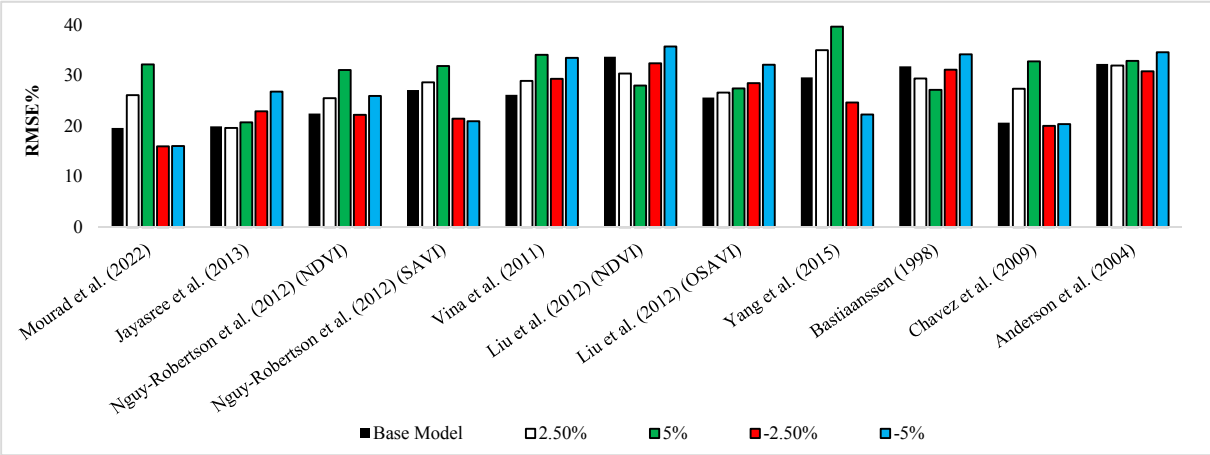

Figure 8. RMSE% for all scenarios used in sensitivity analysis estimating LAI using the UAS platform

3.4.2 Crop Height Estimation Analysis

The RMSE% change for Hc estimation using all RS platforms, as shown in Figure 9 and Figures B1 to B4, has a high sensitivity for most of the models, excluding the models by Costa-Filho et al. (2021) and Anderson et al. (2004). The relatively same changes in RMSE% (same sensitivity) were noticed in all RS platforms, where the trend of the changes suggested a better performance when the independent variables were decreased and lower performance when the independent variables were increased. This indicates that the independent variables (VIs and LAI) were overestimated.

The RMSE% for Hc estimation using the UAS platform models showed a higher sensitivity to positive changes, suggesting a tendency to overestimate Hc when VIs increase. The analysis indicates that UAS-based Hc models are more accurate under negative scenarios. Other platforms, like the UAS, showed a broad range of RMSE%. The results highlight significant sensitivity to both positive and negative changes, with models showing increased errors, particularly under positive scenarios.

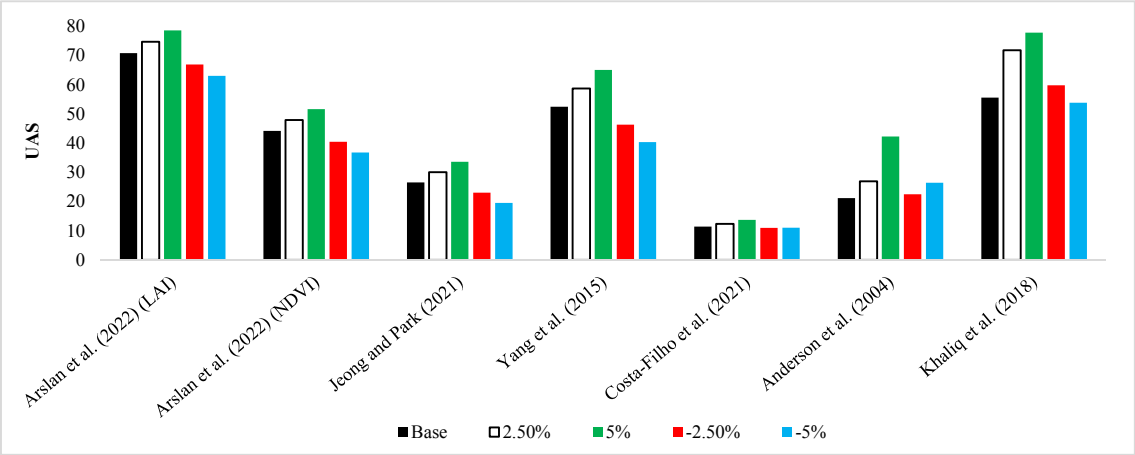

Figure 9. RMSE% for all scenarios used in sensitivity analysis estimating Hc using the UAS platform

3.4.3 Crop Fractional Cover Estimation Analysis

Figure 10 shows the change in RMSE% during each scenario in estimating the Fc for the UAS platform, and Figures C1 to C4 in Appendix C show the RMSE% during each scenario in estimating the Fc for the Planet, Landsat, Sentinel-2, and MSR-5 platforms. The models used with the UAS platform show moderate sensitivity with RMSE%, showing slight increases in RMSE% under both positive and negative scenarios, indicating stable performance but a tendency to overestimate Fc when NDVI increases. PlanetDove exhibits higher sensitivity with RMSE%, indicating a significant sensitivity to changes in NDVI values, particularly under positive scenarios. This suggests that PlanetDove's Fc estimation models are less robust compared to UAS. Landsat shows a wide range of RMSE%, indicating higher sensitivity to changes in NDVI values. The results suggest that Landsat's Fc models are highly sensitive, particularly under negative scenarios, where RMSE% increases significantly. Sentinel-2 demonstrates moderate sensitivity with RMSE%, indicating more stable performance but a tendency to overestimate Fc under positive scenarios. The results suggest that Sentinel-2 provides relatively accurate Fc estimates but requires careful calibration. MSR-5, on the other hand, shows the highest sensitivity with RMSE%. The large variation in RMSE% indicates that MSR-5 models estimating the Fc are highly sensitive to changes in NDVI values, particularly under negative scenarios, suggesting the need for further calibration.

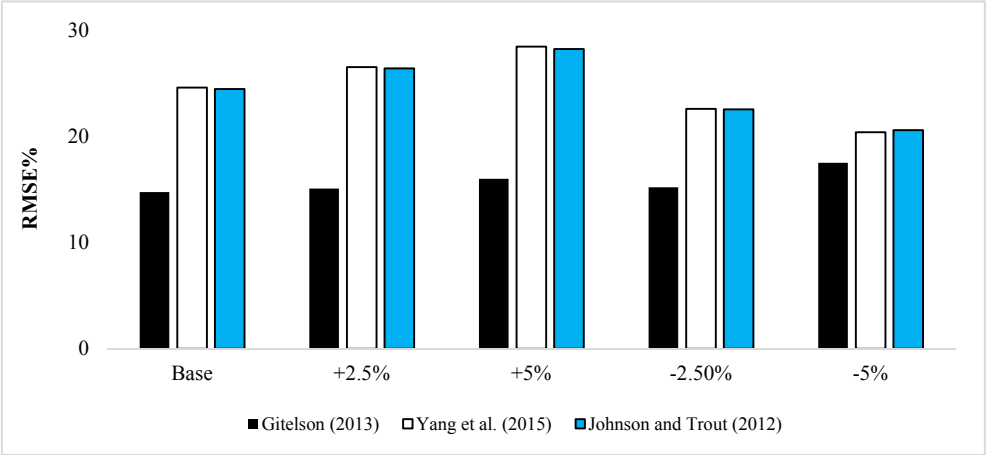

Figure 10. RMSE% for all scenarios used in sensitivity analysis estimating Fc using the UAS platform

3.4.4 Actual Evapotranspiration Estimation Analysis

As shown in Figure 11 and Figures D1 to D4 in Appendix D, most models showed relatively low sensitivity when either increasing or decreasing the independent variable values throughout all RS platforms. The general trend of the performance indicated by the RMSE% varies depending on the model and the RS platform used to

estimate the ETa. Models by Trout and DeJonge (2018) and Neale et al. (1989) showed lower sensitivity compared to other models.

The models used in the UAS platform show low sensitivity, indicating a slight increase in RMSE% under both positive and negative scenarios, indicating stable performance and accurate ETa estimates. PlanetDove exhibited higher sensitivity compared to the UAS, and the results indicate significant sensitivity to changes in VI values, particularly under positive scenarios, suggesting that PlanetDove's ETa imagery needs further calibration to be effectively used in ETa models based on surface reflectance. Landsat showed moderate sensitivity, and the results suggest stable ETa estimates from Landsat, but careful calibration is required under positive scenarios to avoid overestimation. Sentinel-2 demonstrates high sensitivity, indicating that Sentinel-2's ETa models are highly sensitive to changes in VI values, particularly under positive scenarios, suggesting the need for further calibration. MSR-5 shows moderate sensitivity, and the results indicate that MSR-5's ETa estimation models are highly sensitive to changes in VI values, particularly under negative scenarios. The sensitivity analysis across different RS platforms underscores the varying degrees of robustness and accuracy in estimating LAI, Hc, Fc, and ETa. It is important to note that high-resolution platforms like UAS generally demonstrate more stable and accurate estimates, while lower-resolution platforms like PlanetDove and Landsat show higher sensitivity to changes in VI values. This analysis underscores the importance of selecting appropriate RS platforms and calibrating models carefully to ensure accurate agricultural monitoring and water management.

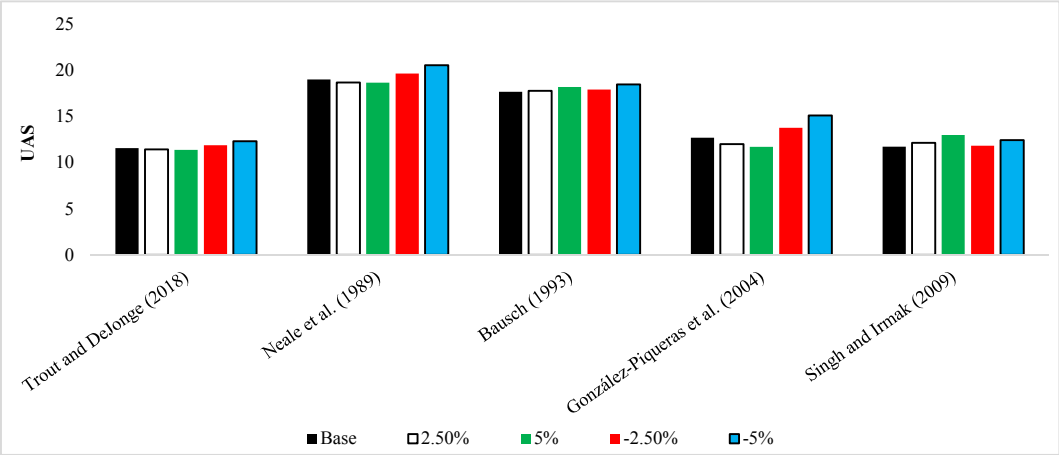

Figure 11. RMSE% for all scenarios used in sensitivity analysis estimating ETa using the UAS platform

4. Conclusions and Recommendations

This study comprehensively analyzed various RS platforms for estimating CBPCs and ETa for maize fields in northeastern Colorado, U.S.A. Its findings highlight several key points. Firstly, the accuracy of VIs estimation varied significantly among the evaluated RS platforms. The RS data from the UAS platform showed the highest accuracy in estimating VIs such as NDVI, OSAVI, and SAVI. The high spatial resolution of UAS and the fact that surface reflectance values were acquired closer to the ground surface allowed for a more detailed canopy assessments, contributing to its high performance. Other satellite platforms, including PlanetDove, Sentinel-2, and Landsat showed slightly less accuracy, although still providing valuable insights with relatively high performance. These platforms offer broader coverage and frequent revisit times, making them practical for regional-scale monitoring and long-term agricultural assessments.

Secondly, the estimation of CBPCs, including LAI, Hc, and Fc, demonstrated that models developed using VIs from the UAS platform provided the most accurate estimates. The high-resolution data captured by UAS proved to be more sensitive to crop canopy structure and health variations. Other platforms followed in accuracy, with each showing strengths depending on specific conditions and crop stages. The influence of environmental conditions on the performance of RS models was significant. Locally calibrated models, which consider the specific environmental conditions of the study area, performed better than those developed in different environmental contexts. These results underscore the importance of site-specific calibration for improving model accuracy. The MSR-5 radiometer, despite being a standard for evaluating surface reflectance and vegetation indices, showed suboptimal performance in estimating CBPCs and ETa in this study. This result could be

attributed to the type of models used, which were developed using different RS sensors/platforms, predominantly space-borne and airborne satellites with different spectral and spatial resolutions.

Thirdly, the estimation of Kcb and ETa revealed that the accuracy varied among the different RS data from platforms used, with UAS-based models again showing higher performance. However, satellite-based estimates were also within acceptable error margins, demonstrating their utility in providing reliable data for large-scale agricultural management. Sensitivity analysis indicated that slight variations in VIs could lead to significant changes in CBPCs and ETa estimates. This result highlights the need for local accurate calibration and validation of RS models to ensure their reliability and accuracy.

Fourthly, the study underscores the potential of advanced RS technologies, particularly UAS, in enhancing agriculture practices and water use. The accurate estimation of CBPCs and ETa can inform better irrigation scheduling, leading to optimized water use and improved crop yields. This fact has significant implications for water resource management in agriculture, particularly in regions facing water scarcity and climatic variability. The analysis of LAI, Hc, Fc, and ETa across various RS platforms reveals distinct performance variations. UAS consistently provided more accurate and reliable estimates across all parameters. Sentinel-2 and Planet platforms showed moderate reliability and potential for good performance under specific conditions. Landsat had the highest variability and generally less reliable estimates, while MSR-5's performance was less consistent and lower than UAS. The results highlight the importance of selecting appropriate RS platforms based on specific study requirements to ensure accurate estimations.

The performance of RS platforms improved significantly during the late crop growth stages compared to the early stages for all parameters. This improvement is attributed to the more stable and developed canopy structure in the late stages, providing clearer crop surface multispectral signals to the RS platforms. Higher spatial resolution platforms like UAS, Planet, and MSR-5 demonstrated better performance when the canopy was less dense during the early stages. However, all platforms showed improved accuracy in the late stages, with UAS remaining the most reliable and stable across both growth stages.

In summary, the choice of an RS platform for agricultural monitoring depends on different characteristics of the RS platform, including spatial, spectral, and temporal resolutions. The UAS, with its very high spatial resolution, is ideal for detailed field-level analysis, capturing fine-scale variability in VIs. However, its limited temporal resolution necessitates frequent flights, which may not be feasible for large-scale applications. On the other hand, Planet provides daily revisit times, making it suitable for monitoring rapid changes in crop conditions, although its lower spatial resolution compared to UAS might miss finer details. Sentinel-2 offers a balance between spatial and temporal resolution, suitable for regional-scale studies, while Landsat's longer revisit time and broader coverage makes it ideal for large-scale environmental monitoring.

Agricultural stakeholders should consider integrating high-resolution UAS data into their monitoring systems for more accurate and reliable results. The higher accuracy of UAS in estimating VIs and CBPCs can lead to more accurate and timely agricultural management decisions. Despite their slightly lower accuracy compared to UAS, other platforms are important to be used due to their broad coverage and frequent revisit times. These platforms are particularly useful for regional-scale monitoring. Models for estimating CBPCs and ETa should be calibrated using local data to account for specific environmental conditions. This local sensor-data calibration will enhance the accuracy and applicability of the CBPCs and ETa models across different regions. Future studies should focus on the comprehensive validation of RS models across different crop types and environmental conditions. This will help in developing robust models that can be generalized to various agricultural settings.

Given the significant differences between controlled experimental conditions and real-world water management scenarios, it is crucial to develop a practical method for estimating ETa in operational irrigation districts. This study demonstrates the potential of using high-resolution RS platforms (e.g., unmanned aerial systems), which have shown superior imagery reflectance/temperature accuracy and derived products for the estimation of CBPCs and ETa. For operational water management, we recommend an approach based on the principle of optimum data acquisition, calibration, and utilization. These high-resolution multispectral data can be used to calibrate and validate models at key crop growth stages, while other RS platforms (i.e., satellites) can provide continuous monitoring due to their frequent revisit times. This hybrid approach will allow water managers to effectively monitor ETa by combining the detailed accuracy of UAS data with the broader and more frequent coverage of satellite platforms. By implementing this method, water managers in minor and major irrigation districts can optimize irrigation scheduling and potentially reduce water usage, contributing to more sustainable water resource management practices.

References

Adams, J. E., & Arkin, G. F. (1977). A light interception method for measuring row crop ground cover. *Soil Science Society of America Journal, 41*(4), 789-792. https://doi.org/10.2136/sssaj1977.03615995004100040037x

Aeberli, A., Johansen, K., Robson, A., Lamb, D. W., & Phinn, S. (2021). Detection of banana plants using multi-temporal multispectral UAV imagery. *Remote Sensing, 13*(11), 2123. https://doi.org/10.3390/rs13112123

Anderson, M. C., Neale, C. M. U., Li, F., Norman, J. M., Kustas, W. P., Jayanthi, H., & Chavez, J. (2004). Upscaling ground observations of vegetation water content, canopy height, and leaf area index during SMEX02 using aircraft and Landsat imagery. *Remote Sensing of Environment, 92*(4), 447-464. https://doi.org/10.1016/j.rse.2004.03.019

Arslan, İ., Topakcı, M., & Demir, N. (2022). Monitoring maize growth and calculating plant heights with Synthetic Aperture Radar (SAR) and optical satellite images. *Agriculture, 12*(6), 800. https://doi.org/10.3390/agriculture12060800

Atzberger, C. (2013). Advances in remote sensing of agriculture: Context description, existing operational monitoring systems and major information needs. *Remote Sensing, 5*(2), 949-981. https://doi.org/10.3390/rs5020949

Baret, F., & Guyot, G. (1991). Potentials and limits of vegetation indices for LAI and APAR assessment. *Remote Sensing of Environment, 35*(2-3), 161-173. https://doi.org/10.1016/0034-4257(91)90009-U

Bastiaanssen, W. G. M. (1998). *Remote sensing in water resources management: The state of the art*. International Irrigation Management Institute.

Bausch, W. C. (1993). Soil background effects on reflectance-based crop coefficients for corn. *Remote Sensing of Environment, 46*(2), 213-222. https://doi.org/10.1016/0034-4257(93)90096-G

Bégué, A., Arvor, D., Bellon, B., Betbeder, J., De Abelleyra, D., Ferraz, R., ... Verón, S. (2018). Remote sensing and cropping practices: A review. *Remote Sensing, 10*(1), 99. https://doi.org/10.3390/rs10010099

Calera, A., Campos, I., Osann, A., D'Urso, G., & Menenti, M. (2017). Remote sensing for crop water management: From ET modelling to services for the end users. *Sensors, 17*(5), 1104. https://doi.org/10.3390/s17051104

Chávez, J. L., Gowda, P. H., Howell, T. A., Neale, C. M. U., & Copeland, K. S. (2009). Estimating hourly crop ET using a two-source energy balance model and multispectral airborne imagery. *Irrigation Science, 28*, 79-91. https://doi.org/10.1007/s00271-009-0177-9

Chávez, J. L., Torres-Rua, A., Woldt, W., Zhang, H., Robertson, C., Marek, G., … Neale, C. M. U. (2020). A Decade of Unmanned Aerial Systems in Irrigated Agriculture in the Western U.S. *ASABE Applied Engineering in Agriculture, 36*(4), 423-436. https://doi.org/10.13031/aea.13941

Chávez, J. L., Zhang, H., Brown, A. J., Andales, A., & Costa-Filho, E. (2024). Maize Evapotranspiration Estimates Using Planet Dove Mini-Satellites and Field-Level InfraRed Thermometers. *Applied Engineering in Agricultural, 40*(1), 69-78. https://doi.org/10.13031/aea.15703

Costa-Filho, E., Chávez, J. L., Zhang, H., & Andales, A. A. (2021). An optimized surface aerodynamic temperature approach to estimate maize sensible heat flux and evapotranspiration. *Agricultural and Forest Meteorology, 311*, 108683. https://doi.org/10.1016/j.agrformet.2021.108683

Evans, R. G., & Sadler, E. J. (2008). Methods and technologies to improve efficiency of water use. *Water Resources Research, 44*(7). https://doi.org/10.1029/2007WR006200

Galán-Martín, Á., Vaskan, P., Antón, A., Esteller, L. J., & Guillén-Gosálbez, G. (2017). Multi-objective optimization of rainfed and irrigated agricultural areas considering production and environmental criteria: a case study of wheat production in Spain. *Journal of Cleaner Production, 140*, 816-830. https://doi.org/10.1016/j.jclepro.2016.06.099

Gao, B. C. (1996). NDWI—A normalized difference water index for remote sensing of vegetation liquid water from space. *Remote Sensing of Environment, 58*(3), 257-266. https://doi.org/10.1016/S0034-4257(96)00067-3

Gitelson, A. A. (2013). Remote estimation of crop fractional vegetation cover: the use of noise equivalent as an indicator of performance of vegetation indices. *International Journal of Remote Sensing, 34*(17), 6054-6066. https://doi.org/10.1080/01431161.2013.793868

Gonzalez-Piqueras, J., Calera, A., Gilabert, M. A., Cuesta, A., & De la Cruz Tercero, F. (2004, February). Estimation of crop coefficients by means of optimized vegetation indices for corn. *Remote Sensing for Agriculture, Ecosystems, and Hydrology V* (Vol. 5232, pp. 110-118). SPIE. https://doi.org/10.1117/12.511317

Huete, A. R. (1988). A soil-adjusted vegetation index (SAVI). *Remote sensing of Environment, 25*(3), 295-309. https://doi.org/10.1016/0034-4257(88)90106-X

Jafarbiglu, H., & Pourreza, A. (2022). A comprehensive review of remote sensing platforms, sensors, and applications in nut crops. *Computers and Electronics in Agriculture, 197*, 106844. https://doi.org/10.1016/j.compag.2022.106844

Jamieson, P. D., Porter, J. R., & Wilson, D. R. (1991). A test of the computer simulation model ARCWHEAT1 on wheat crops grown in New Zealand. *Field Crops Research, 27*(4), 337-350. https://doi.org/10.1016/0378-4290(91)90040-3

Jayasree, G., Lingaiah, D., Reddy, D. R., & Rao, S. N. (2013). Relationship between biophysical parameters and normalized difference vegetation index in maize. *Journal of Agrometeorology, 15*(2), 120-125. https://doi.org/10.54386/jam.v15i2.1457

Jeong, C. H., & Park, J. H (2021). Analysis of Growth Characteristics Using Plant Height and NDVI of Four Waxy Corn Varieties Based on UAV Imagery. *Korean J. Remote Sens., 37*(4), 733-745.

Johnson, L. F., & Trout, T. J. (2012). Satellite NDVI assisted monitoring of vegetable crop evapotranspiration in California's San Joaquin Valley. *Remote Sensing, 4*(2), 439-455. https://doi.org/10.3390/rs4020439

Kamble, B., Irmak, A., Hubbard, K., & Gowda, P. (2013). Irrigation scheduling using remote sensing data assimilation approach. *Advances in Remote Sensing, 2*(03), 258. https://doi.org/10.4236/ars.2013.23028

Karthikeyan, L., Chawla, I., & Mishra, A. K. (2020). A review of remote sensing applications in agriculture for food security: Crop growth and yield, irrigation, and crop losses. *Journal of Hydrology, 586*, 124905. https://doi.org/10.1016/j.jhydrol.2020.124905

Kasampalis, D. A., Alexandridis, T. K., Deva, C., Challinor, A., Moshou, D., & Zalidis, G. (2018). Contribution of remote sensing on crop models: A review. *Journal of Imaging, 4*(4), 52. https://doi.org/10.3390/jimaging4040052

Khaliq, A., Musci, M. A., & Chiaberge, M. (2018). Analyzing relationship between maize height and spectral indices derived from remotely sensed multispectral imagery. *2018 IEEE Applied Imagery Pattern Recognition Workshop (AIPR)* (pp. 1-5). IEEE. https://doi.org/10.1109/AIPR.2018.8707373

Leys, C., Ley, C., Klein, O., Bernard, P., & Licata, L. (2013). Detecting outliers: Do not use standard deviation around the mean, use absolute deviation around the median. *Journal of Experimental Social Psychology, 49*(4), 764-766. https://doi.org/10.1016/j.jesp.2013.03.013

Liu, J., Pattey, E., & Jégo, G. (2012). Assessment of vegetation indices for regional crop green LAI estimation from Landsat images over multiple growing seasons. *Remote Sensing of Environment, 123*, 347-358. https://doi.org/10.1016/j.rse.2012.04.002

Miller, J. (1991). Reaction time analysis with outlier exclusion: Bias varies with sample size. *The Quarterly Journal of Experimental Psychology Section A, 43*(4), 907-912. https://doi.org/10.1080/14640749108400962

Moran, M. S., Inoue, Y., & Barnes, E. M. (1997). Opportunities and limitations for image-based remote sensing in precision crop management. *Remote sensing of Environment, 61*(3), 319-346. https://doi.org/10.1016/S0034-4257(97)00045-X

Mourad, R., Jaafar, H., Anderson, M., & Gao, F. (2020). Assessment of leaf area index models using harmonized landsat and sentinel-2 surface reflectance data over a semi-arid irrigated landscape. *Remote Sensing, 12*(19), 3121. https://doi.org/10.3390/rs12193121

Neale, C. M., Bausch, W. C., & Heermann, D. F. (1990). Development of reflectance-based crop coefficients for corn. *Transactions of the ASAE, 32*(6), 1891-1900. https://doi.org/10.13031/2013.31240

Nguy-Robertson, A., Gitelson, A., Peng, Y., Viña, A., Arkebauer, T., & Rundquist, D. (2012). Green leaf area index estimation in maize and soybean: Combining vegetation indices to achieve maximal sensitivity. *Agronomy Journal, 104*(5), 1336-1347. https://doi.org/10.2134/agronj2012.0065

Olivera-Guerra, L., Merlin, O., Er-Raki, S., Khabba, S., & Escorihuela, M. J. (2018). Estimating the water budget components of irrigated crops: Combining the FAO-56 dual crop coefficient with surface temperature and vegetation index data. *Agricultural Water Management, 208*, 120-131. https://doi.org/10.1016/j.agwat.2018.06.014

Payero, J. O., Neale, C. M. U., & Wright, J. L. (2004). Comparison of eleven vegetation indices for estimating plant height of alfalfa and grass. *Applied Engineering in Agriculture, 20*(3), 385-393. https://doi.org/10.13031/2013.16057

Planet Team. (2017). *Planet Application Program Interface: In Space for Life on Earth*. San Francisco, CA. Retrieved from https://api.planet.com

Rondeaux, G., Steven, M., & Baret, F. (1996). Optimization of soil-adjusted vegetation indices. *Remote Sensing of Environment, 55*(2), 95-107. https://doi.org/10.1016/0034-4257(95)00186-7

Rouse, J. W., Haas, R. H., Schell, J. A., & Deering, D. W. (1974). Monitoring vegetation systems in the Great Plains with ERTS. *NASA Spec. Publ, 351*(1), 309.

Saadi, S. (2018). *Spatial estimation of actual evapotranspiration and irrigation volumes using water and energy balance models forced by optical remote sensing data (VIS/NIR/TIR)* (Doctoral dissertation, Université Paul Sabatier-Toulouse III, Université de Carthage, Tunisie).

Shanmugapriya, P., Rathika, S., Ramesh, T., & Janaki, P. (2019). Applications of remote sensing in agriculture—A review. *Int. J. Curr. Microbiol. Appl. Sci., 8*(01), 2270-2283. https://doi.org/10.20546/ijcmas.2019.801.238

Singh, R. K., & Irmak, A. (2009). Estimation of crop coefficients using satellite remote sensing. *Journal of Irrigation and Drainage Engineering, 135*(5), 597-608. https://doi.org/10.1061/(ASCE)IR.1943-4774.0000052

Sishodia, R. P., Ray, R. L., & Singh, S. K. (2020). Applications of remote sensing in precision agriculture: A review. *Remote Sensing, 12*(19), 3136. https://doi.org/10.3390/rs12193136

Thenkabail, P. S., Lyon, J. G., & Huete, A. (2018). Advances in hyperspectral remote sensing of vegetation and agricultural crops. *Fundamentals, Sensor Systems, Spectral Libraries, and Data Mining for Vegetation* (pp. 3-37). CRC Press. https://doi.org/10.1201/9781315164151-1

Trout, T. J., & DeJonge, K. C. (2018). Crop water use and crop coefficients of maize in the great plains. *Journal of Irrigation and Drainage Engineering, 144*(6), 04018009. https://doi.org/10.1061/(ASCE)IR.1943-4774.0001309

Viña, A., Gitelson, A. A., Nguy-Robertson, A. L., & Peng, Y. (2011). Comparison of different vegetation indices for the remote assessment of green leaf area index of crops. *Remote Sensing of Environment, 115*(12), 3468-3478. https://doi.org/10.1016/j.rse.2011.08.010

Wardlow, B. D., Egbert, S. L., & Kastens, J. H. (2007). Analysis of time-series MODIS 250 m vegetation index data for crop classification in the US Central Great Plains. *Remote Sensing of Environment, 108*(3), 290-310. https://doi.org/10.1016/j.rse.2006.11.021

Yang, Y., Long, D., Guan, H., Liang, W., Simmons, C., & Batelaan, O. (2015). Comparison of three dual-source remote sensing evapotranspiration models during the MUSOEXE-12 campaign: Revisit of model physics. *Water Resources Research, 51*(5), 3145-3165. https://doi.org/10.1002/2014WR015619

Appendix A

Leaf Area Index Estimation Sensitivity Analysis

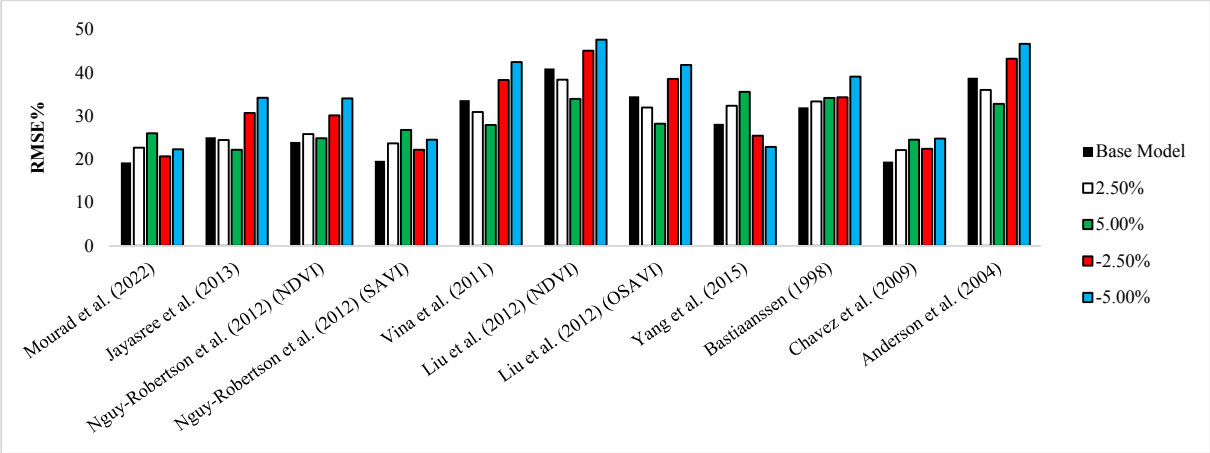

Figure A1. RMSE% for all scenarios used in sensitivity analysis estimating LAI using Planet platform

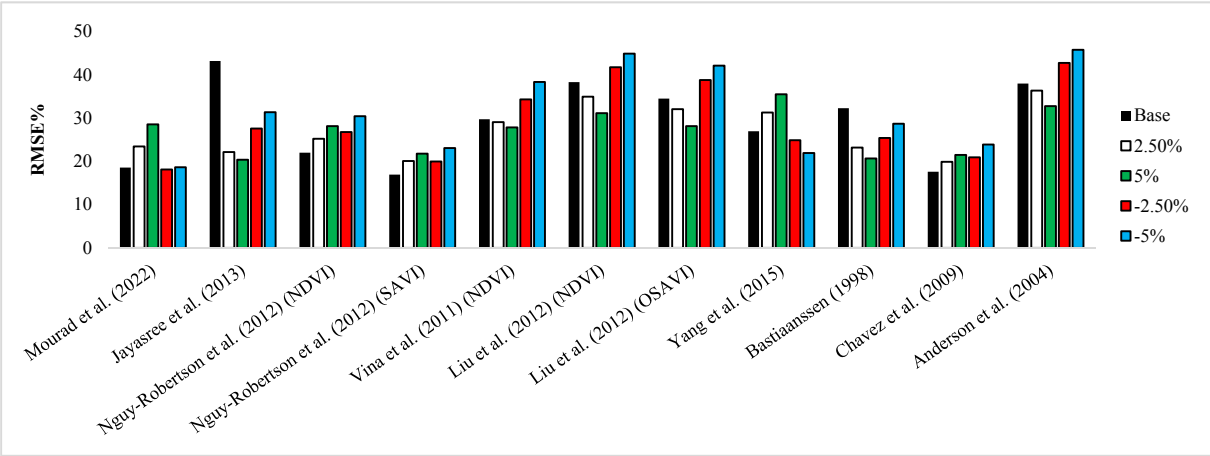

Figure A2. RMSE% for all scenarios used in sensitivity analysis estimating LAI using Landsat platform

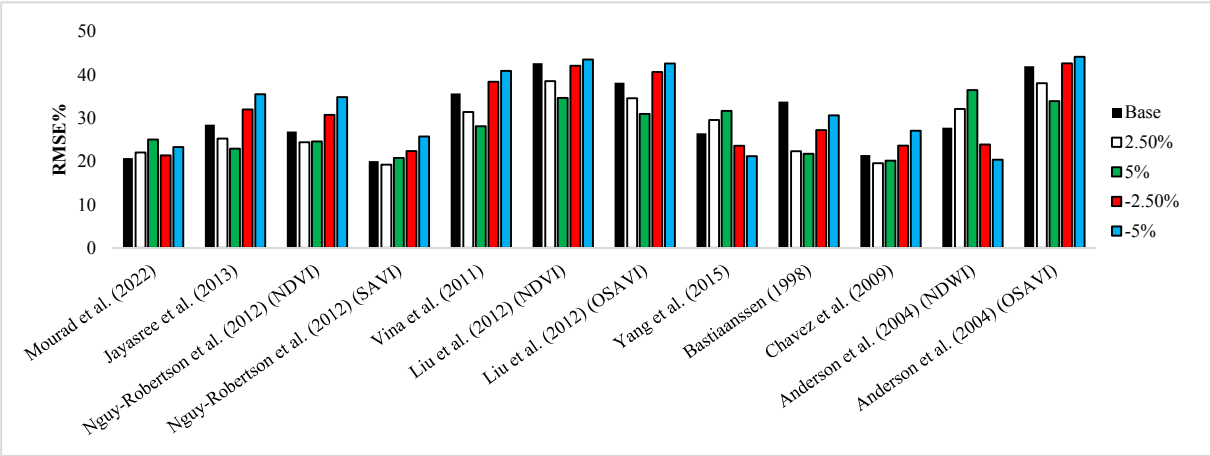

Figure A3. RMSE% for all scenarios used in sensitivity analysis estimating LAI using Sentinel-2 platform

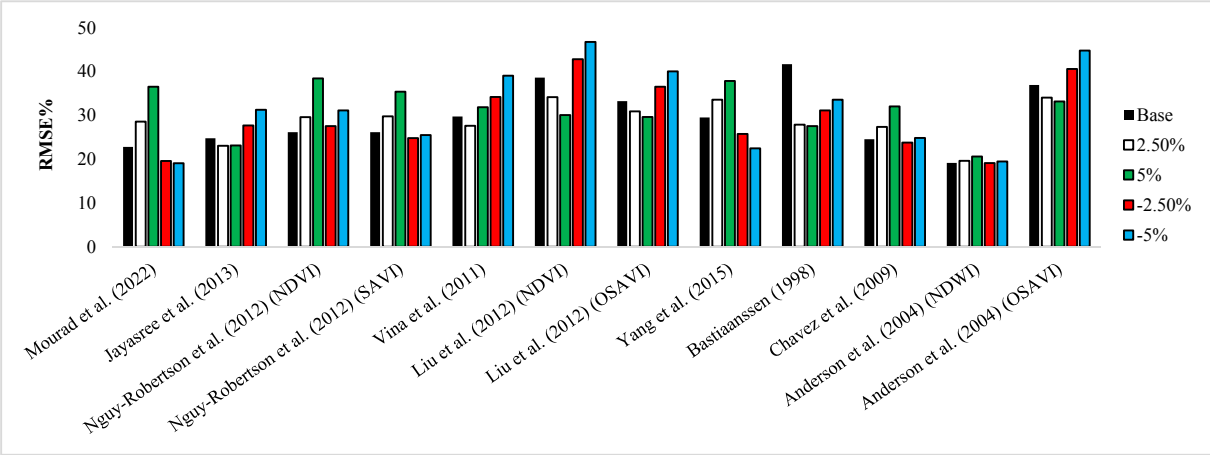

Figure A4. RMSE% for all scenarios used in sensitivity analysis estimating LAI using MSR-5 platform

Appendix B

Crop Height Estimation Sensitivity Analysis

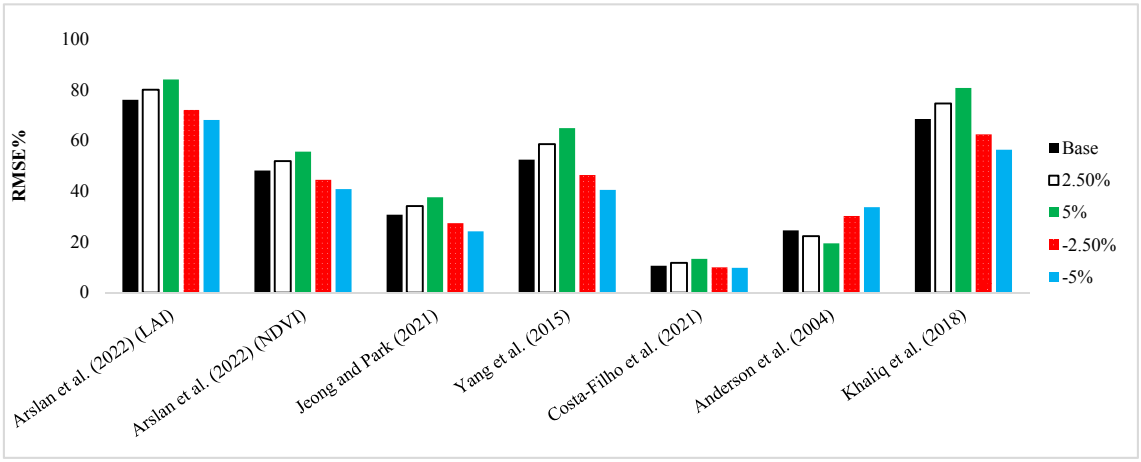

Figure B1. RMSE% for all scenarios used in sensitivity analysis estimating Hc using Planet platform

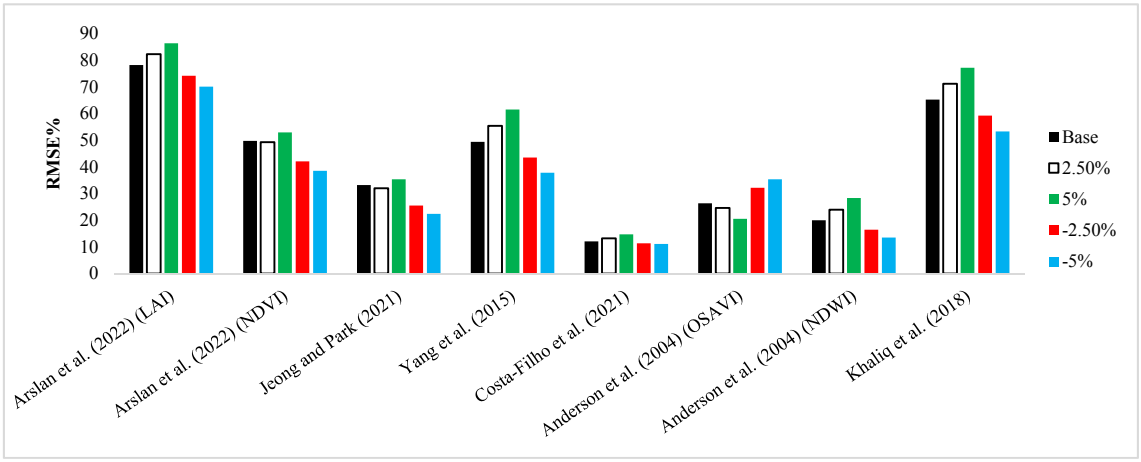

Figure B2. RMSE% for all scenarios used in sensitivity analysis estimating Hc using Landsat platform

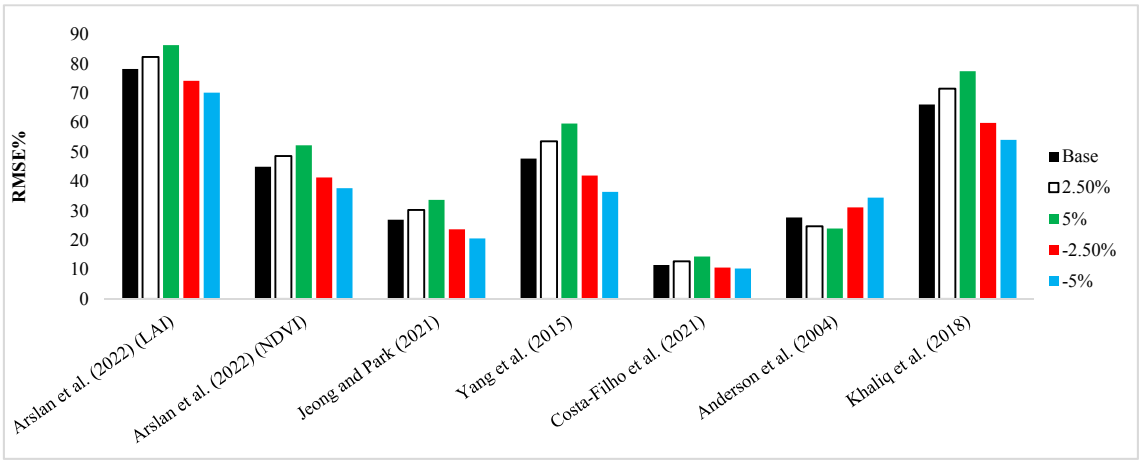

Figure B3. RMSE% for all scenarios used in sensitivity analysis estimating Hc using Sentinel-2 platform

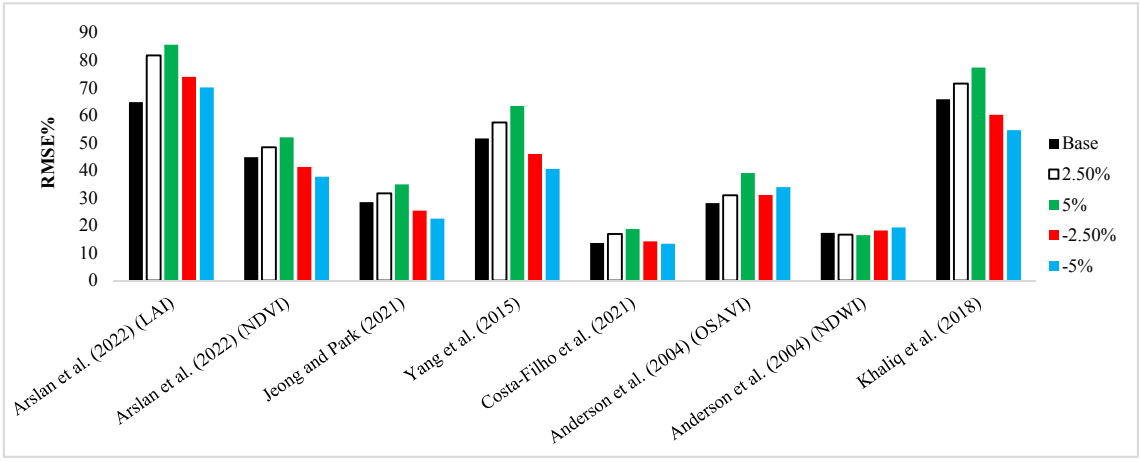

Figure B4. RMSE% for all scenarios used in sensitivity analysis estimating LAI using MSR-5 platform

Appendix C

Fractional Vegetation Cover Estimation Sensitivity Analysis

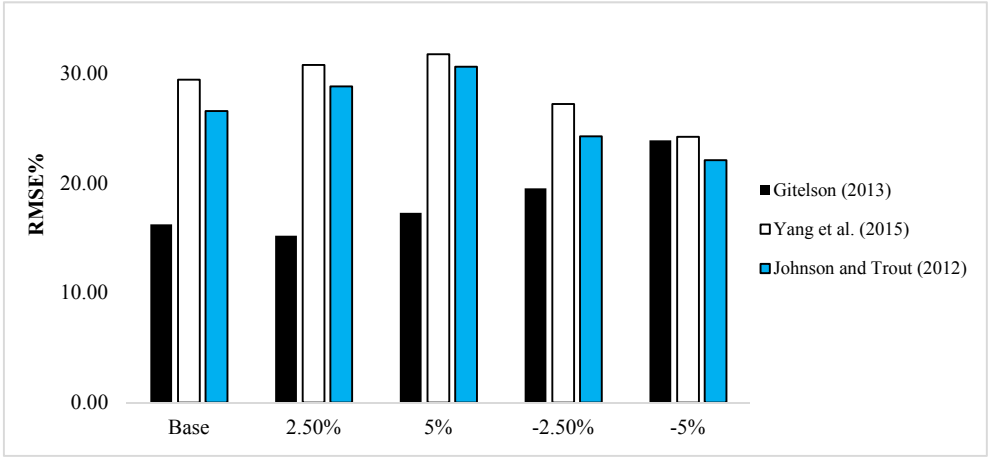

Figure C1. RMSE% for all scenarios used in sensitivity analysis estimating Fc using Planet platform

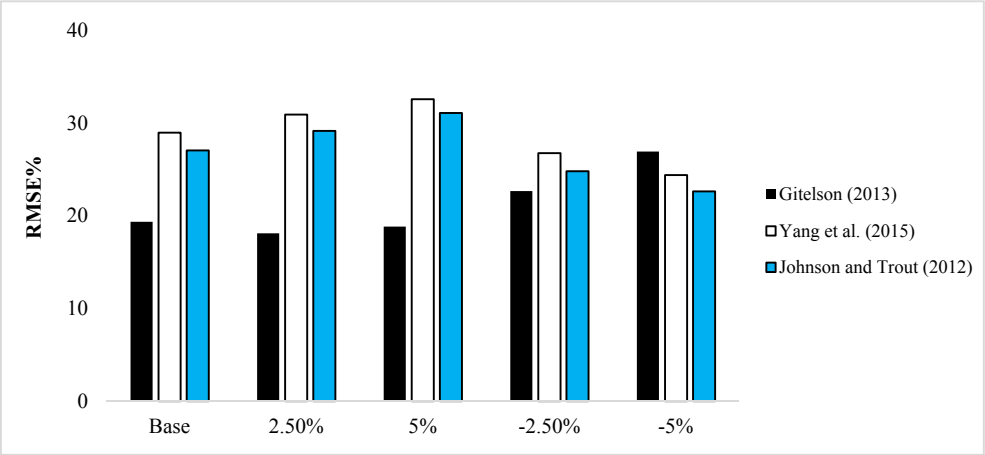

Figure C2. RMSE% for all scenarios used in sensitivity analysis estimating Fc using Landsat platform

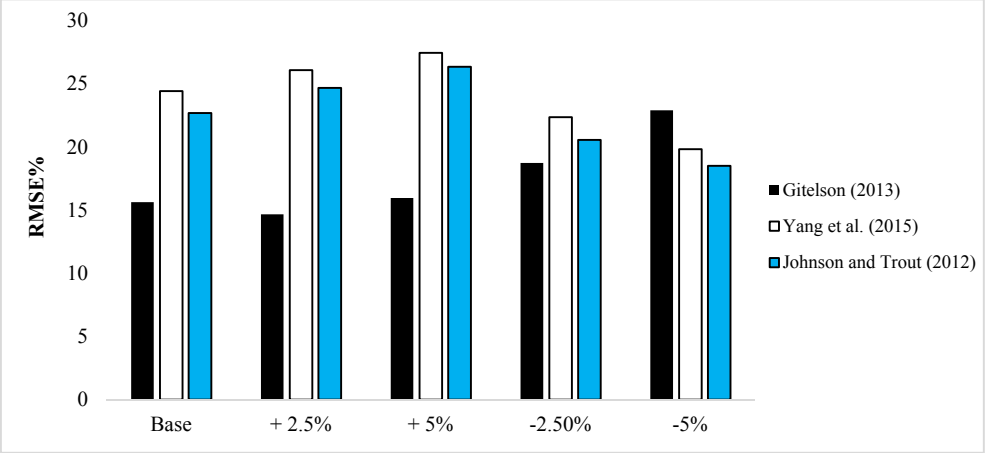

Figure C3. RMSE% for all scenarios used in sensitivity analysis estimating Fc using Sentienl-2 platform

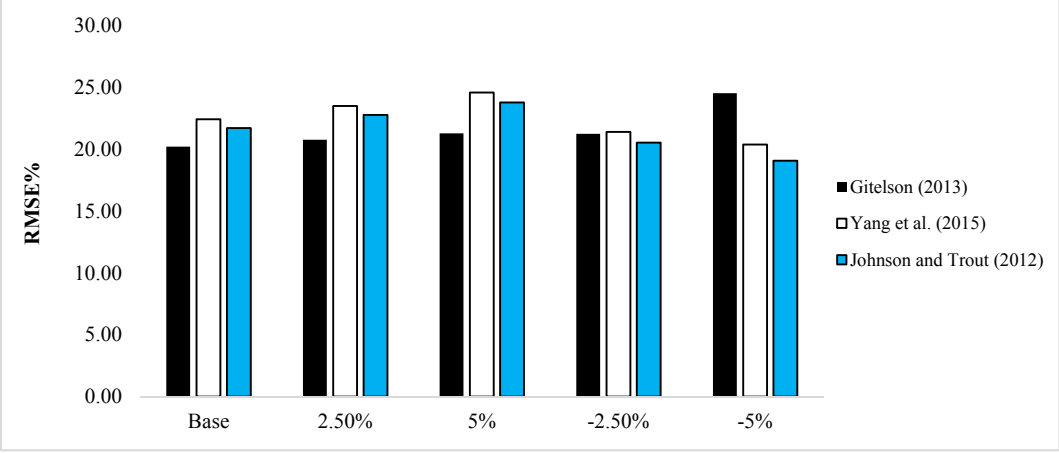

Figure C4. RMSE% for all scenarios used in sensitivity analysis estimating Fc using MSR-5 platform

Appendix D

Actual Evapotranspiration Estimation Sensitivity Analysis

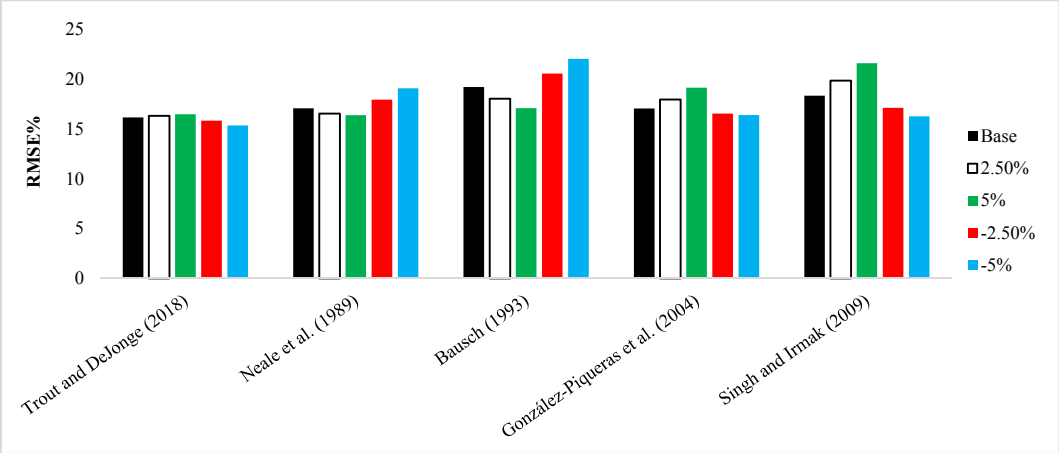

Figure D1. RMSE% for all scenarios used in sensitivity analysis estimating ETa using Planet platform

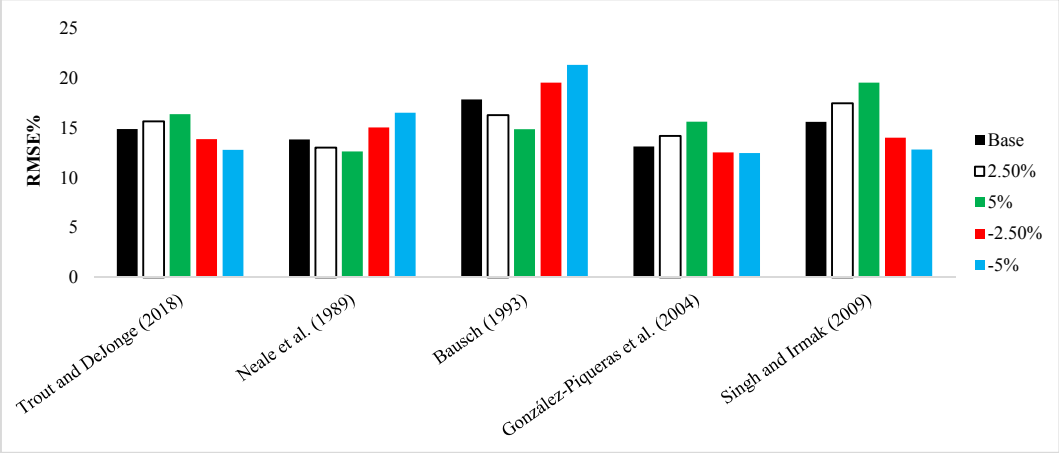

Figure D2. RMSE% for all scenarios used in sensitivity analysis estimating ETa using Landsat platform

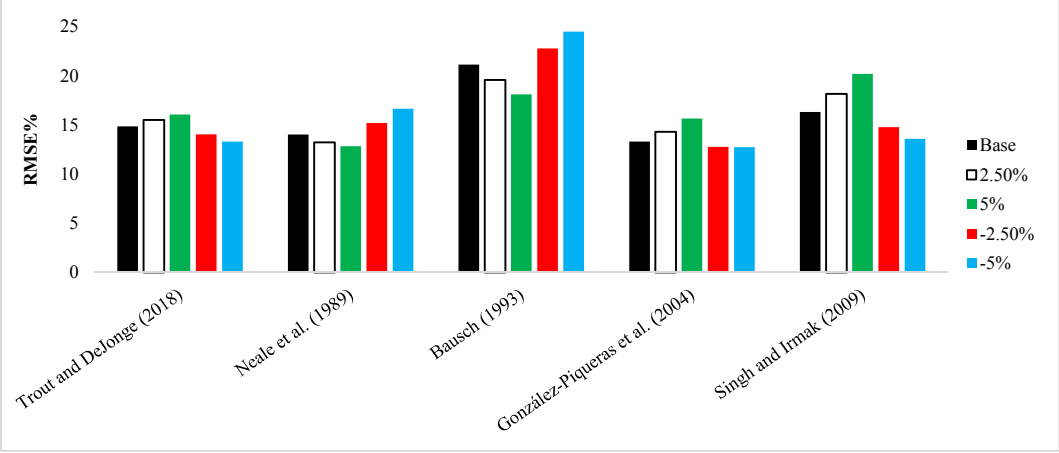

Figure D3. RMSE% for all scenarios used in sensitivity analysis estimating ETa using Sentinel-2 platform

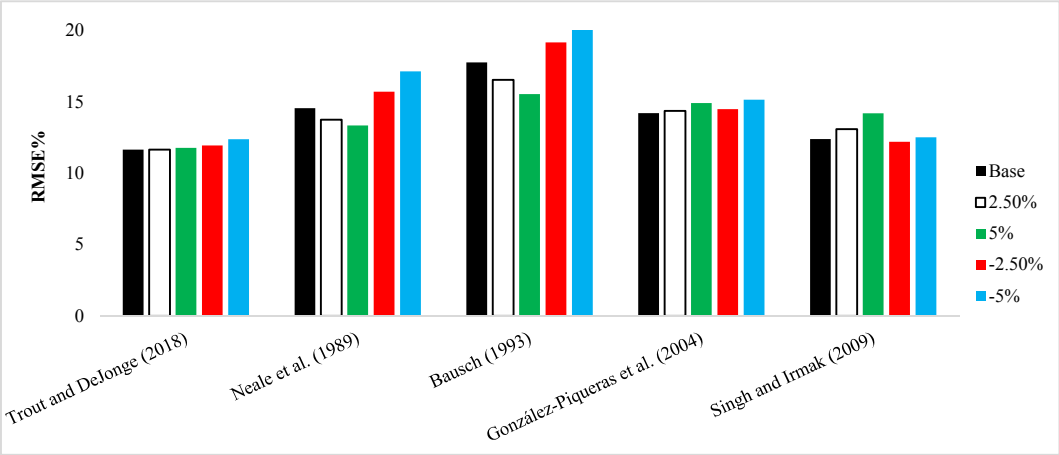

Figure D4. RMSE% for all scenarios used in sensitivity analysis estimating ETa using MSR-5 platform

Acknowledgments

We greatly appreciate the valuable contributions of Jon Altenhofen (Northern Water) who managed the irrigation treatments and provided the atmometer and crop fractional cover data, and to Dr. Huihui Zhang and Kevin Yemoto (USDA-ARS, Fort Collins, CO, USA) for providing the UAS data. We would also like to thank the USDA ARS LIRF manager and summer students who took care of the field agronomics and operations.

Authors Contributions

Dr. Chávez was responsible for the study design, data collection, oversight and revising. Mr. Al-Majali was responsible for data processing, methodology application, data analysis and interpretation, and manuscript writing. All authors read and approved the final manuscript.

Funding

This project was in part funded by an FY23 grant from the Colorado Water Center's CSU Competitive Grant Program and by the National Science Foundation NSF-MCA Award 2120906.

Competing Interests

The authors declare that they have no known competing financial interests or personal relationships that could have appeared to influence the work reported in this paper.

Informed Consent

Obtained.

Ethics Approval

The Publication Ethics Committee of the Canadian Center of Science and Education. The journal's policies adhere to the Core Practices established by the Committee on Publication Ethics (COPE).

Provenance and Peer Review

Not commissioned; externally double-blind peer-reviewed.

Data Availability Statement

The data supporting this study's findings are available on request from the corresponding author. The data are not publicly available due to privacy or ethical restrictions.

Data Sharing Statement

No additional data are available.